8

Bransfield Strait, Antarctic Peninsula
Active Extension behind a Dead Arc

Lawrence A. Lawver, Randall A. Keller, Martin R. Fisk, and Jorge A. Strelin

ABSTRACT

Bransfield Strait is a marginal basin landward of the South Shetland Trench. It lies between the South Shetland Islands and the tip of the Antarctic Peninsula and is an example of an extensional basin formed by rifting within a continental volcanic arc. The Antarctic Peninsula is the product of at least 200 m.y. of subduction with the majority of the exposed rocks related to continental arc volcanism older than 20 Ma. Volcanism in Bransfield Strait started by 0.3 Ma and continues today. This new volcanism maintains some of the chemical signatures of the old arc volcanism but also has signatures transitional between arc rocks and backarc basin rocks. On the basis of high heat flow, active volcanism, extensional faulting, and earthquake fault plane mechanisms, Bransfield Strait is an active extensional basin forming within the Antarctic Peninsula. Seismic refraction work in Bransfield Strait indicates some thinning of continental crust, but the basin itself is underlain by as much as 30 km of anomalous crustal material. The observed extension seems to be confined to Bransfield Strait, which is bounded by the landward projections of the Hero and Shackleton fracture zones. The present extension in Bransfield Rift started less than 4 m.y. ago, and possibly less than 1.5 m.y. ago, following the demise of the Antarctic–Phoenix spreading center (ANT–PHO ridge), which ceased spreading about 4 Ma. Apparent, continued subduction at the South Shetland Trench after the ANT–PHO ridge stopped spreading may occur as trench rollback. The amount of trench rollback should be comparable to the amount of extension in Bransfield Strait.

Lawrence A. Lawver • Institute for Geophysics, University of Texas at Austin, Austin, Texas 78759-8397. *Randall A. Keller and Martin R. Fisk* • College of Oceanic and Atmospheric Sciences, Oregon State University, Corvallis, Oregon 97331-5503. *Jorge A. Strelin* • Departmento de Ciencias de la Tierra, Instituto Antartico Argentino, Buenos Aires, Argentina.

Backarc Basins: Tectonics and Magmatism, edited by Brian Taylor, Plenum Press, New York, 1995.

1. INTRODUCTION

Bransfield Strait (Fig. 8.1) is an example of a basin that formed by rifting within a continental volcanic arc. For most of the past 200 m.y., the Antarctic Peninsula (Fig. 8.1) has been the site of subduction of oceanic lithosphere that formed at spreading centers in the South Pacific (Tanner *et al.*, 1982; Barker and Dalziel, 1983; Pankhurst, 1983; Hole *et al.*, 1991). Major plate motions in the vicinity of Bransfield Strait and the Antarctic Peninsula are well constrained by magnetic anomaly patterns preserved on the Antarctic, Pacific, Scotia, and former Phoenix plates (Barker, 1982). At about 4 Ma, the Antarctic–Phoenix (ANT–PHO) spreading center ceased spreading and the remnant Phoenix plate was incorporated into the Antarctic plate. Previous authors have referred to the remnant plate as the Aluk plate (Herron and Tucholke, 1976; Barker, 1982; Mayes *et al.*, 1990; GRAPE Team, 1990), the Drake plate (Barker, 1982; Mayes *et al.*, 1990), and/or the Phoenix plate (Barker, 1982; Larter and Barker, 1991). Larson and Chase (1972) used the terms *Phoenix lineations*, *Phoenix model*, and *Phoenix plate*, and related the terms to the Phoenix Islands found in the central Pacific Ocean. Although the Phoenix lineations and the Phoenix Islands both lie on the Pacific plate, they assigned the term *Phoenix plate* to the "southern" half of the Pacific–Phoenix spreading center and traced a possible Pacific–Phoenix fracture zone from the Phoenix lineations to the Eltanin fracture zone system's intersection with the present-day Pacific–Antarctic Ridge. They correctly pointed out that "It is unlikely that the Phoenix plate corresponded to the Antarctic plate until about 85 m.y.B.P. ...," because "Antarctica and New Zealand did not begin to separate until just prior to anomaly 32." The designation

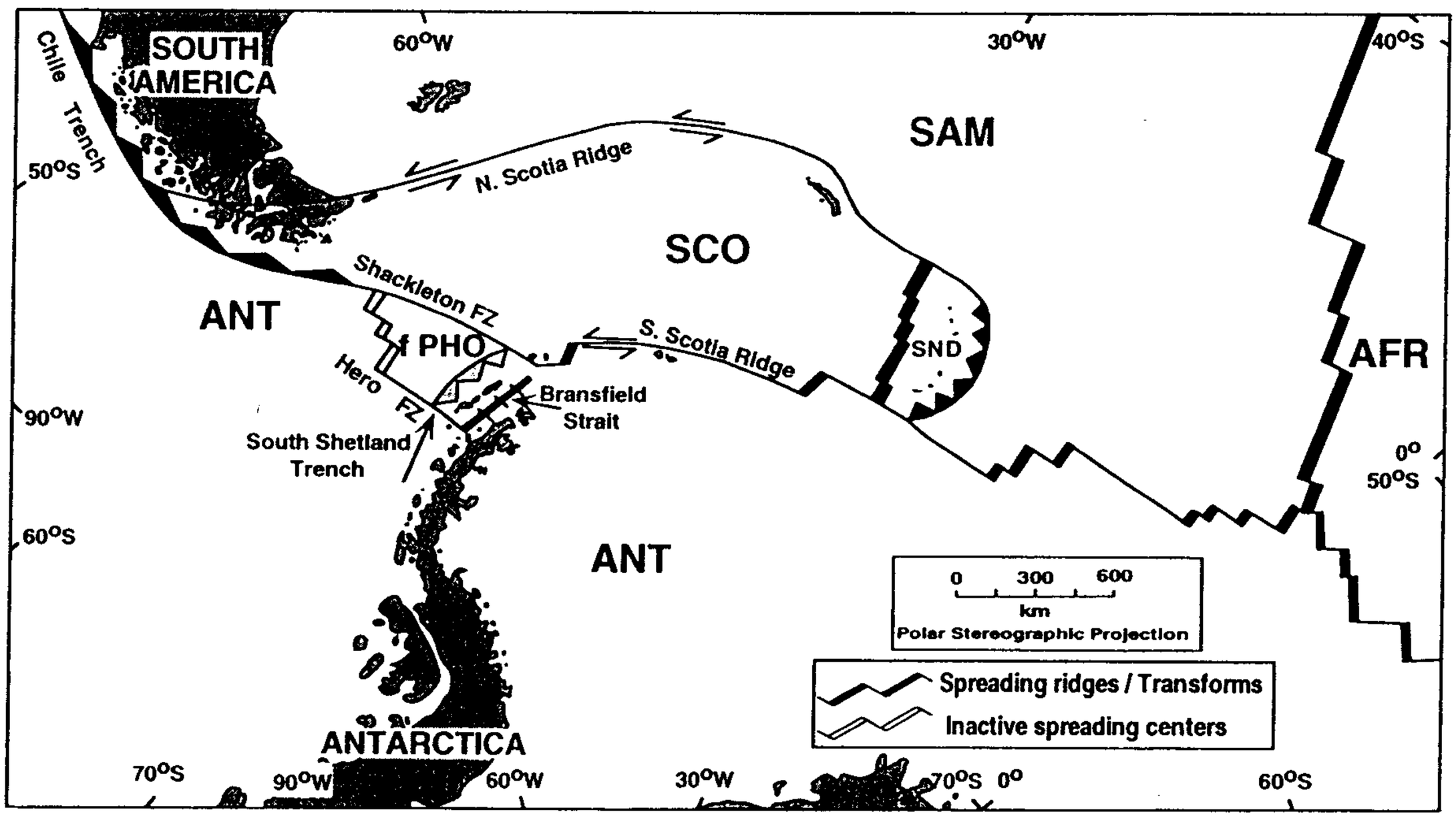

FIGURE 8.1. Present-day, polar stereographic map of the regional tectonic setting of the Bransfield Strait area modified from the Tectonic Map of the Scotia Arc [1985; British Antarctic Survey Sheet (Miscellaneous) 3]. Abbreviations for the major plates are AFR = Africa, ANT = Antarctic, f PHO = former Phoenix, SCO = Scotia, and SND = Sandwich plate. The South Shetland plate lies between the South Shetland Trench and the active rift shown in Bransfield Strait. Double arrows indicate direction of strike-slip motion along the North and South Scotia ridges. Active trenches are shown as black. The South Shetland Trench is shown shaded.

Phoenix plate for the remnant plate off Bransfield Strait is therefore tectonically most accurate and should take precedence.

Seismic reflection and refraction work, gravity, magnetics, and heat flow data, and the history and composition of volcanism on the peninsula and in Bransfield Strait place constraints on the processes associated with the formation of Bransfield Strait as a marginal basin. Recent dredges from new sites in Bransfield Strait (Keller *et al.*, 1994) will soon be analyzed and will give better control on active basin formation.

2. REGIONAL TECTONIC SETTING

Present-day plate boundaries are indicated in Fig. 8.1. Plate reconstructions (Barker, 1982; Mayes *et al.*, 1990) suggest that at least a thousand kilometers of the Phoenix plate have been subducted beneath Bransfield Strait since 50 Ma. Between 50 and 43 Ma, a segment of the ANT-PHO spreading center between the Tharp and Heezen fracture zones (Fig. 8.2) was subducted (Barker, 1982). At 20 Ma, the active South Shetland Trench was

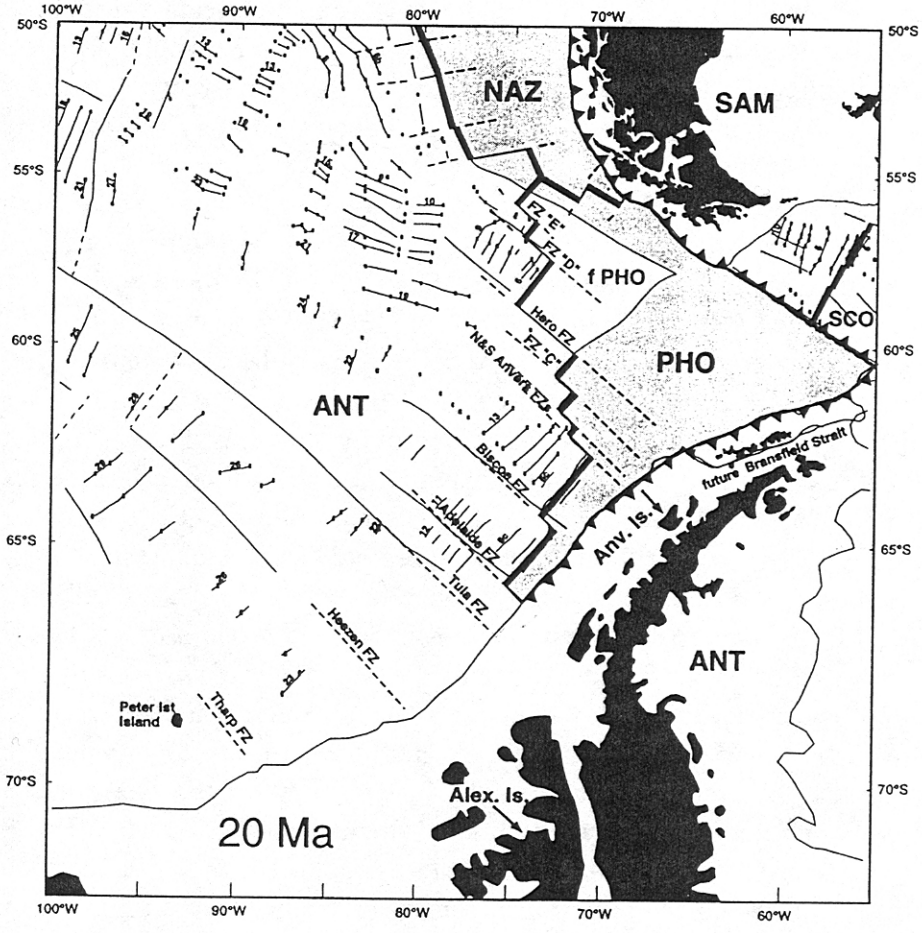

FIGURE 8.2. Reconstruction of Southeast Pacific and Antarctic Peninsula regions for 20 Ma. The reconstruction is based on the PLATES database. Dashed fracture zones and spreading centers are taken from Larter and Barker (1991). Plate abbreviations are as in Fig. 8.1: NAZ = Nazca plate, PHO = Phoenix, Alex. = Alexander Island, Anv. = Anvers Island. Magnetic anomaly picks are shown as small squares. Magnetic lineations connect the small squares. Rifting in Bransfield Strait has been closed up so that the South Shetland Islands are closer to the Antarctic Peninsula than they are at present. The shaded region is the seafloor that was subducted since 20 Ma.

nearly twice the length it was after about 14 Ma, when the sections between the Adelaide and Anvers fracture zones were subducted. Through time, additional segments of the ridge were subducted to the northeast, until about 4 Ma, when the spreading center immediately southwest of the Hero fracture zone reached the trench (Barker, 1982). The last segment of the ANT-PHO spreading center (between the Hero and Shackleton fracture zones) was then abandoned offshore of the trench and the last remnant of the Phoenix plate (f PHO, Fig. 8.2) became part of the Antarctic plate.

Until 4 Ma, the subducting plate was decoupled from the overriding plate as the lower Phoenix plate slid beneath the upper Antarctic plate. As the Phoenix–Antarctic spreading centers were subducted, the subducted slab continued to sink, leaving in its wake a slab window (Hole and Larter, 1993). After 4 Ma, when the last Phoenix–Antarctic spreading center southwest of the Hero fracture zone was subducted, the remnant, unsubducted Phoenix plate (former Phoenix plate = f PHO) was frozen in place between the Hero and Shackleton fracture zones. Whether this resulted in the subducted Phoenix slab, to the southwest of the Hero fracture zone, to also be frozen in place with respect to the underlying mantle or if it continued to sink independently is a matter of speculation. If the subducted slab to the southwest of the Hero fracture zone continued to sink but the slab beneath Bransfield Strait was held in place by the f PHO, then there would have to be tearing or differential motion along the subducted section of the Hero fracture zone, and there would be no slab window beneath Bransfield Strait. On the other hand, if the slab beneath Bransfield Strait is detached from the f PHO and sinking, then there should be deep seismicity and evidence of a slab window in the geochemistry.

Other marginal basins along the outer edge of the Antarctic Peninsula may have formed in response to the subduction of ridge segments to the southwest of the Hero fracture zone (Gambôa and Maldonado, 1990), although none of these basins seem to have reached the advanced state of Bransfield Strait. GEOSAT gravity data from 72°S to the northeast along the western margin of the Antarctic Peninsula (Lawver *et al.*, 1993) show a marginal gravity low that extends from George VI Sound (70°S, 70°W) between Alexander Island and the peninsula, to the southern edge of Anvers Island at 65°W. This gravity signature is similar to the one seen in Bransfield Strait. Single-channel seismic reflection lines from along this margin (Anderson *et al.*, 1990) show features that resemble inner shelf troughs and old forearc basins that might be interpreted as precursors to Bransfield Strait, although these basins do not show any evidence for extension. Larter and Barker (1989) suggested that the forearc to the south of Bransfield Strait was simply uplifted and eroded but not extended after ridge-trench collision.

The age of the subducted Phoenix plate at the South Shetland Trench (Fig. 8.1) increases from 14 Ma in the southwest near the Hero fracture zone to 23 Ma in the northeast near the Shackleton fracture zone (Barker, 1982). Between the Hero and Shackleton fracture zones, there are at least two additional fracture zones, D and E (Fig. 8.2). Their landward extensions would cross the neovolcanic zone of Bransfield Strait at about 59°W (FZ D) and 57°50′W (FZ E). At the trench, the age difference across FZ D is 3 m.y.; across FZ E, 3.5 m.y. (Larter and Barker, 1991).

Presently, the subducted slab can be detected beneath the South Shetland Islands (Grad *et al.*, 1993) dipping at an angle of 25° to the southeast (Fig. 8.3), although there is virtually no seismic activity associated with the lower plate slab (Pelayo and Wiens, 1989). This may be explained by either slow, aseismic descent of the slab, or the slab beneath the South Shetland Islands and Bransfield Strait is frozen in place such that there is no detectable motion of the slab relative to the asthenosphere below it. If the lower or

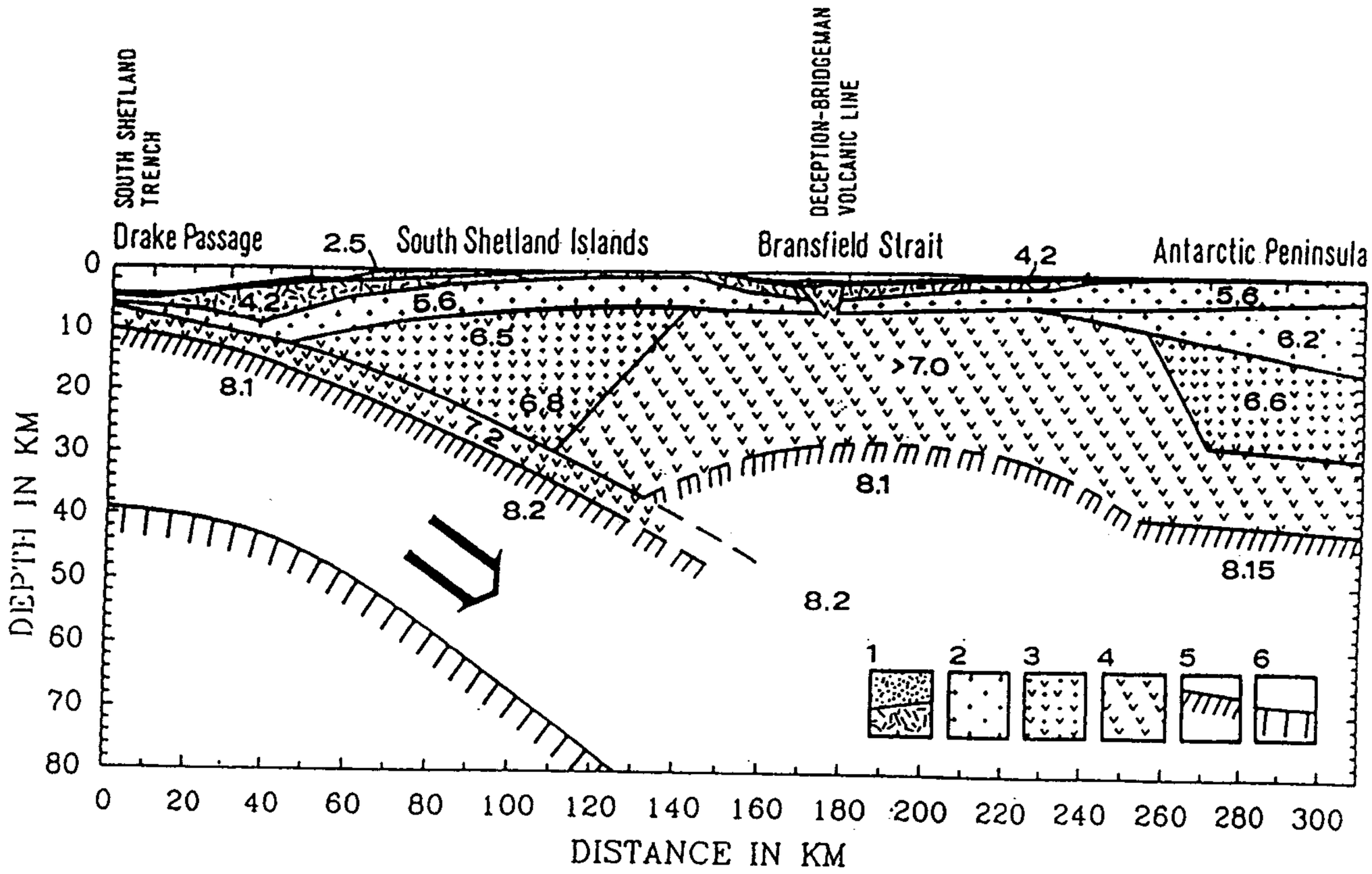

FIGURE 8.3. Seismic model of the lithosphere from the deep-ocean side of the South Shetland Islands through Bransfield Strait and onto the Antarctic Peninsula taken from Grad *et al.* (1993). The symbols used are (1) sediments, $v_p = 2.5–4.2$ km s^{-1}, (2) upper crust, $v_p = 5.4–6.3$ km s^{-1}, (3) middle crust, $v_p = 6.4–6.8$ km s^{-1}, (4) lower crust and high-velocity body in Bransfield Strait, $v_p > 7.0$ km s^{-1}, (5) Moho boundary, $v_p > 8.0$ km s^{-1}, (6) reflection boundary in the lower lithosphere. Notice that the volcanic line is not centered in the middle of Bransfield Strait.

subducted plate remains attached to the f PHO, then any extension in the upper plate must be accompanied by trench rollback. While some may argue that trench rollback is evidence for subduction, we make the distinction that in this case, if the lower plate is still attached to the Antarctic plate, it cannot be subducting with respect to itself, and the independent South Shetland plate must therefore be moving with respect to the lower plate. This in turn produces the observed rollback or seaward motion of the trench. If the slab has broken from the former Phoenix plate or is sinking along a hinge line at the trench, then there should be deep seismicity and there would not be evidence for deformation of the accretionary wedge.

Prior to the demise of the ANT–PHO spreading center, the Shackleton FZ to the north of Bransfield Strait was the boundary between the Antarctic and Phoenix plates on one side and the Scotia plate on the other (Fig. 8.1). Seafloor spreading stopped in the western Scotia Sea immediately to the east of the Shackleton FZ at 6 Ma (Barker and Burrell, 1977). At about 4 Ma, when the remaining Phoenix plate became a part of the Antarctic plate, the Scotia–Phoenix plate boundary became part of the Scotia–Antarctic plate boundary. From 4 Ma to recently, the Scotia–Antarctic plate boundary to the north of Bransfield Strait has trended NW-SE (Shackleton fracture zone), while to the east of Bransfield Strait it has trended E-W (South Scotia Ridge). The consequence of this 110° bend in the plate boundary would be compression on the inside of the bend and extension on the outside of the bend. This should produce extension in the North Bransfield Basin, the part of Bransfield Strait between Bridgeman Island (Fig. 8.4) and Clarence Island. Single-channel seismic reflection profiles across the North Bransfield Basin (Lawver and Villinger, 1989) show continentward tilted blocks, reminiscent of the continental extension models of Wernicke

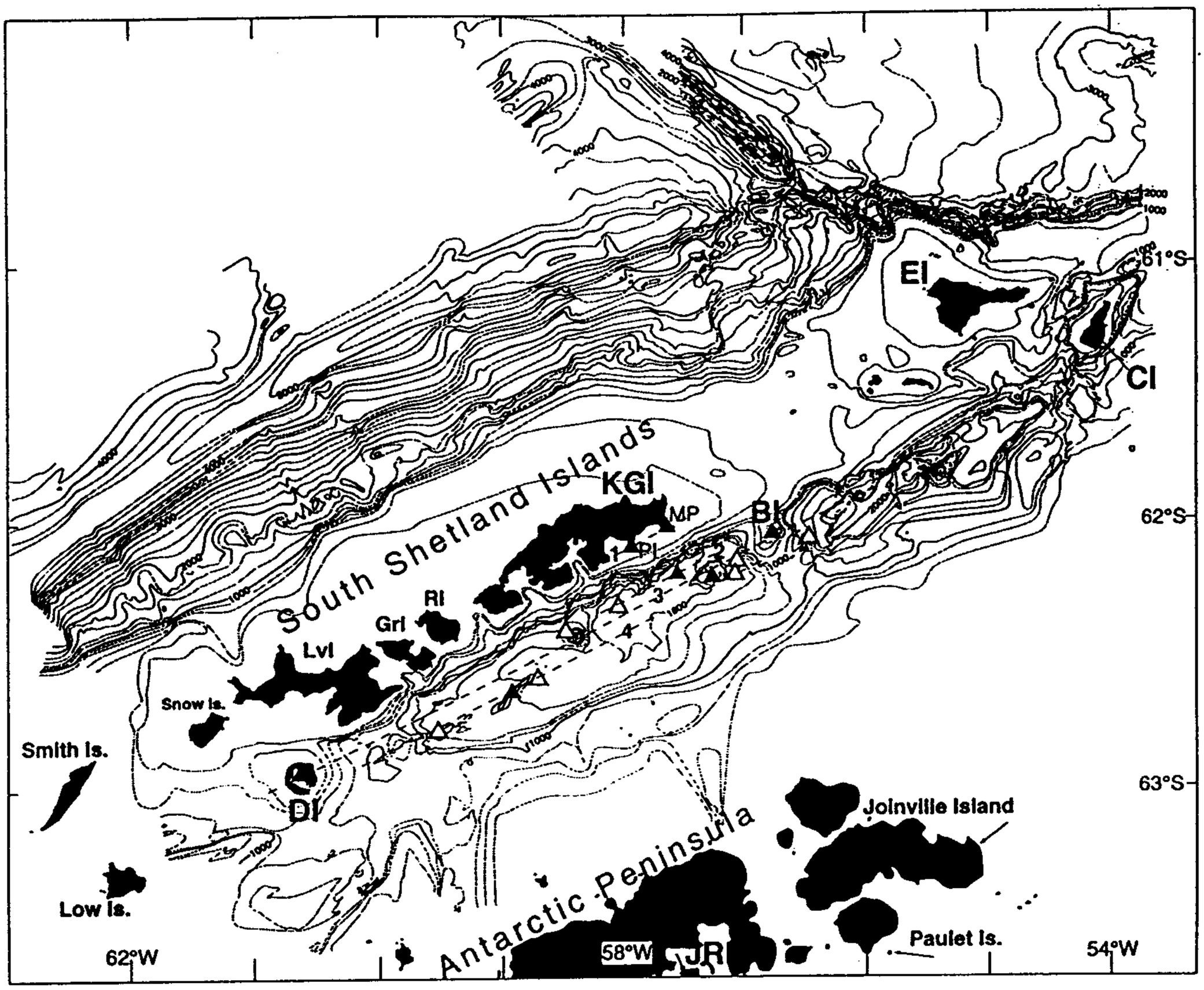

FIGURE 8.4. Bathymetric map of Bransfield Strait region (modified from Klepeis and Lawver, 1994). Bransfield Strait lies between the South Shetland Islands and the Antarctic Peninsula. Contour interval is 200 m, 1000-m contour lines are shown as bold lines and some are labeled. The 1800-m contour southwest of King George Island (KGI) outlines the King George Basin. Solid triangles are locations of submarine and subaerial Quaternary rift-related volcanism that have been sampled and analyzed (Keller *et al.*, 1992). Hollow triangles are submarine locations where fresh, glassy basalts have been recovered (Keller *et al.*, 1994) but not yet analyzed. BI = Bridgman Island, CI = Clarence Island, DI = Deception Island, EI = Elephant Island, GrI = Greenwich Island, JRI = James Ross Island, LvI = Livingston Island, MP = Melville Peak, PI = Penguin Island, and RI = Robert Island. Dashed lines numbered 1 through 4 are parallel or subparallel volcanic lineations, ranging in size from tens of meters in height to 2 km, or more for Deception Island and the submarine volcano south of KGI.

(1981). Evidence for compression includes the extraordinarily steep SW face of Clarence Island which varies from −1200 m to +2300 m in a distance of 10 km or less. The low temperature, high-pressure metamorphics found on Clarence Island and on the eastern half of Elephant Island (Dalziel, 1984) also support the idea of compression and uplift within the bend.

3. TECTONIC SETTING OF BRANSFIELD STRAIT

The strait itself is approximately 100 km wide by 400 km long and is bounded on the northwest by steep normal faults with as much as 4 km of downthrow to the southeast between the South Shetland Islands and the Bransfield basins (Ashcroft, 1972). Birkenmajer (1992) distinguishes between the 100-km-wide Bransfield Strait and a narrowly defined (15–20 km wide) Bransfield rift. From field mapping on King George Island,

Birkenmajer (1992) found fossil evidence that a marine basin existed during the early Eocene (fossiliferous glaciomarine strata from the Kraków Glaciation) and during the Eocene part of the succeeding interglacial time. He reports that during early Oligocene the region was covered by an ice sheet and then later flooded by a shallow sea. Regional uplift caused the area to be above sea level until the late Oligocene when incipient rifting started at the end of the Oligocene (26 to 22 Ma).

The basins of Bransfield Strait are thought to be mainly Quaternary features, although the age of initiation of rifting is poorly constrained. Much of the early faulting is associated with the arc-building period of the peninsula. Evidence for early extension consists of a system of antithetic faults that cut the upper Oligocene and older rocks along the margin of the rift. Arc tension continued through early Miocene when several stages of basaltic to andesitic dyke intrusions occurred between 22 and 20 Ma and at 14 Ma (Birkenmajer, 1992). From the late Miocene to Pliocene there is no evidence of faulting or volcanism within Bransfield Strait. The present Bransfield rift is the site of Pleistocene to Recent, mildly alkaline to calcalkaline volcanic activity.

The present plate configuration in the Bransfield Strait region places the South Shetland Islands on a separate (South Shetland) microplate, bounded on the northwest by the South Shetland Trench and on the southeast by the Bransfield rift. The southeast boundary of Bransfield Strait rises more gently toward the Antarctic Peninsula through a series of widely spaced normal faults (Ashcroft, 1972). The active rift appears to extend 400 km (Gonzalez-Ferran, 1985) from Low Island (Fig. 8.4) above the landward extension of the Hero fracture zone to Clarence Island above the landward extension of the Shackleton fracture zone. Based on GEOSAT/ERS-1 satellite-derived gravity data (Fig. 8.5), Bransfield Strait can be subdivided into three basins: the south, central, and north Bransfield basins. The south Bransfield Basin shows up as a ~100-km-long gravity anomaly trending southwest of Deception Island. The south Bransfield Basin approximately follows the 1000-m contour shown in Larter and Barker (1991, Fig. 8.4). The central Bransfield Basin is a graben up to 2 km deep and roughly 40 km wide by 200 km long that is easily seen on the bathymetric map (Fig. 8.4). It extends from Deception Island to Bridgeman Island and contains the 20- by 50-km, flat-floored King George Basin southeast of King George Island. The north Bransfield Basin is actually the deepest part of Bransfield Strait with a maximum depth over 2740 m and the lowest gravity anomaly, <-30 mgal. The lowest gravity anomaly is not coincident with the deepest part of the basin but is to the northeast toward Clarence Island. If the positive gravity anomalies produced by Deception and Bridgeman Islands (which are relatively young structures) are removed from the GEOSAT data shown in Fig. 8.5, the subdivisions of Bransfield Strait lose their definition and a single major gravity low extends from just south of Low Island to Clarence Island.

The digital bathymetric map (Fig. 8.4) of Bransfield Strait and the nearby region (Klepeis and Lawver, 1994) shows numerous small bathymetric features that appear to be mounds and are lineated, parallel to the basin axis defined by a line through Deception and Bridgeman Islands. Some of these mounds can be seen in Fig. 8.4. There are at least four parallel lines of active and incipient volcanism. The first is discussed by Birkenmajer (1992) and includes Penguin Island, an active cinder cone just off King George Island. This lineation is within the shelf area of the South Shetland Islands. The second line is defined in King George Basin by at least six to eight closed contours indicating circular structures from a few tens of meters in height to a couple of hundred meters. The third line is the main rift axis and includes Deception and Bridgeman Islands and at least two major submarine volcanoes that are up to 1.4 km in height above the seafloor and as much as 8 km in

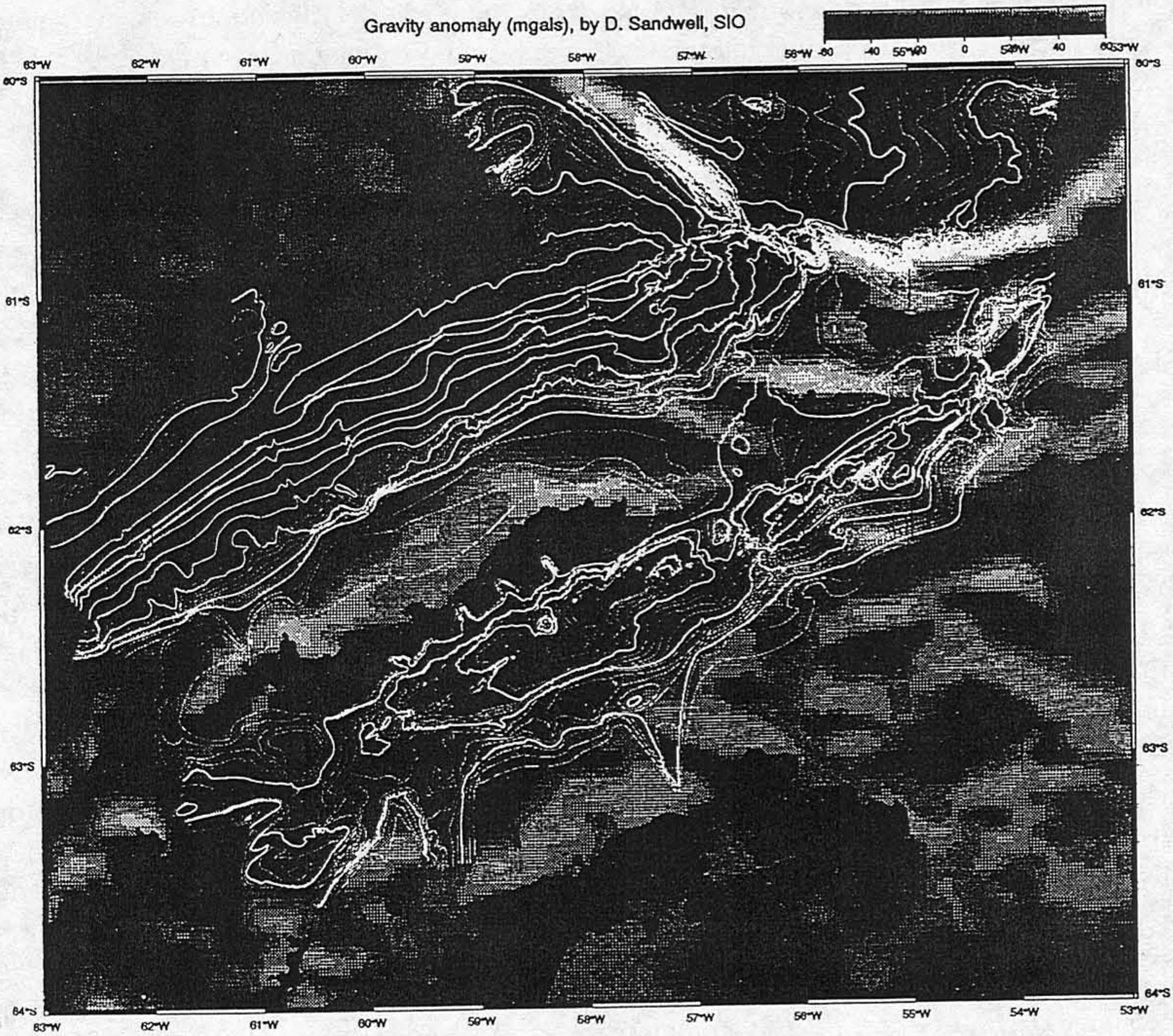

FIGURE 8.5. Geosat/ERS-1 gravity data from Sandwell and Smith (1992) with digital bathymetric data of Klepeis and Lawver (1994) superimposed. The gravity data bar indicates gravity values from <-40 mgal to $>+30$ mgal. Bold white bathymetric contours are shown every 500 m, while thin white contours are observed bathymetry contoured every 100 m. Thin gray contours are interpolated bathymetric data contoured every 100 m. A color version of this figure appears opposite page 311.

diameter. The final volcanic lineation is defined by a ridge (Fig. 8.4), the highest heat flow in King George Basin, and a very recent extrusion at 57°W.

The observed recent faulting (Fig. 8.6) seen in the multichannel seismic data (Barker and Austin, 1994) may define yet a fifth zone of extension and deformation, and although diapirism is suggested, no actual intrusion is observed. Barker and Austin (1994) show an alignment of intracrustal diapirs that trend subparallel to the other neovolcanic zones but in fact diverge from them by about 5°. They suggest that the divergence shows a temporal/spatial evolution of stress in Bransfield Strait, possibly related to the complex plate interactions to the northeast.

4. EARTHQUAKES

Most of the earthquakes in Bransfield Strait are shallow events related to extension and volcanic activity (Fig. 8.7). Deep events in the subducted plate are rare. The vast

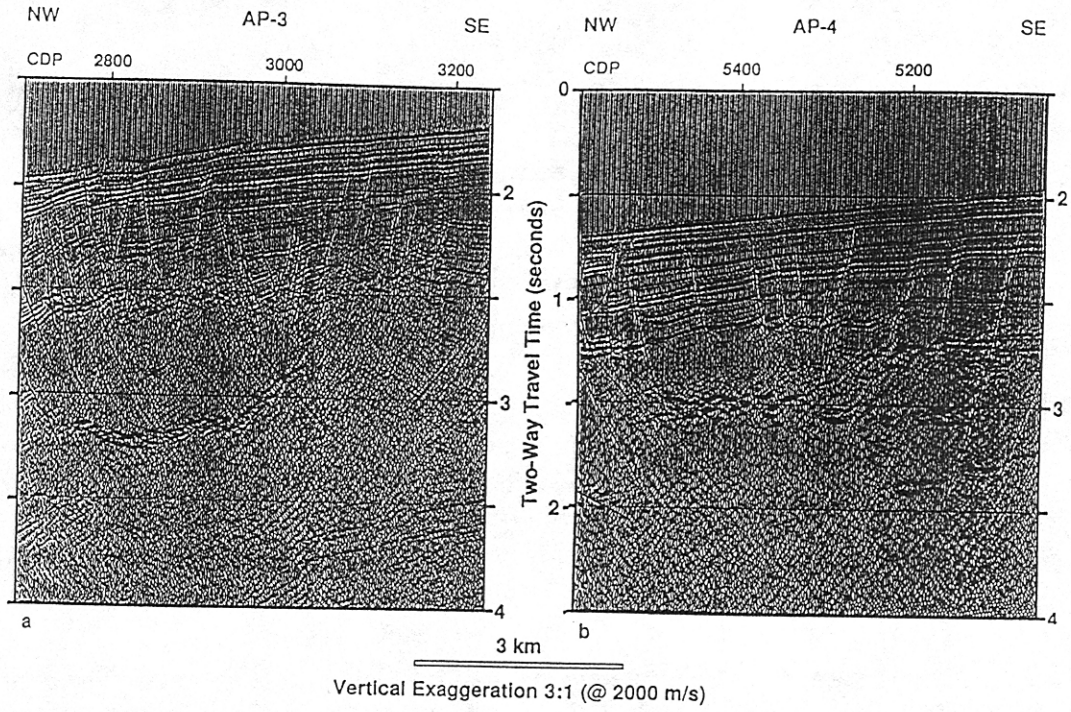

FIGURE 8.6. Seismic cross sections taken from Barker and Austin (1994). Locations shown in Fig. 8.8. Profile shows fan-shaped, normal faulting pattern where the faults reverse their dip about a midpoint (at ~CDP 3000 for 8.6a, ~CDP 5300 for 8.6b). The fault blocks rotate away from the center of the structure, and central faults are confined to the upper part of the section. The inferred diapiric body is unreflective.

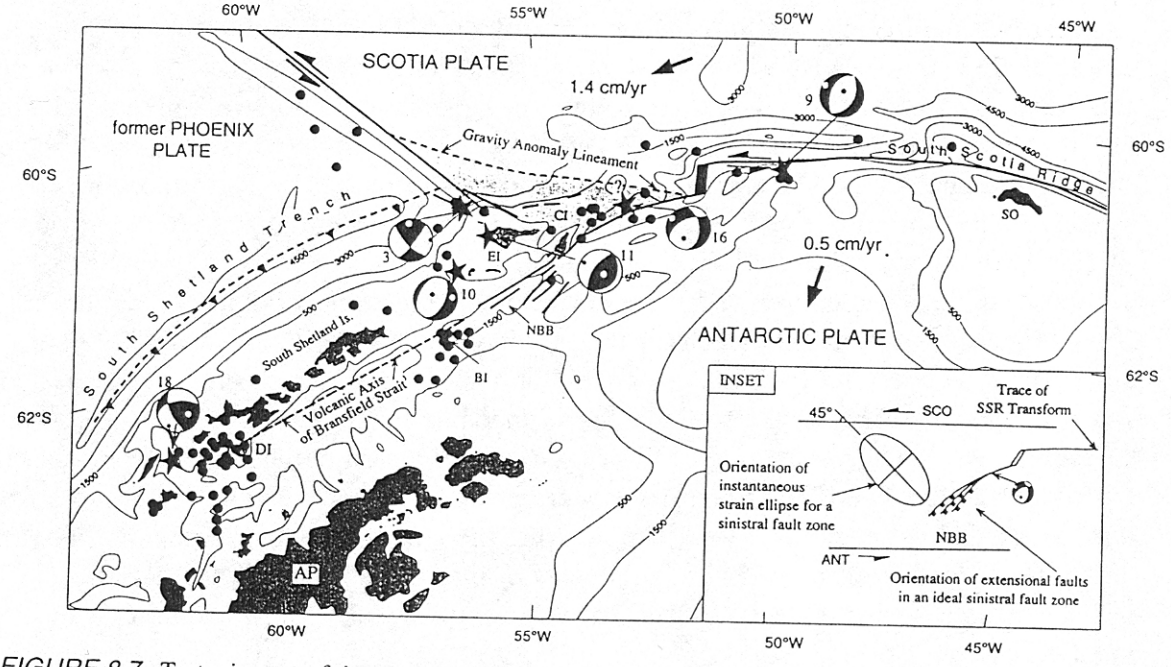

FIGURE 8.7. Tectonic map of the area north of the Antarctic Peninsula (AP) showing interpreted geometry of the plate boundaries between the Shackleton fracture zone and the South Scotia Ridge. EI is Elephant Island, CI is Clarence Island, BI is Bridgeman Island, and NBB is North Bransfield Basin, SSR (inset) is South Scotia Ridge, dashed line labeled BS axis is the volcanic rift axis of Bransfield Strait. Bold lines located north EI/CI represent faults interpreted to parallel the steep scarps of the EI platform's northern margin, bold lines south of EI/CI are the major fault zones taken from Klepeis and Lawver (1994). GEOSAT gravity anomaly is after Sandwell (1992). Circles are earthquake epicenters from the Tectonic Map of the Scotia Arc (1985). Focal mechanisms are for shallow earthquakes from Pelayo and Wiens (1989). Shaded area between GEOSAT gravity anomaly lineament and EI/CI represents a broad zone of tectonic disruption where the Shackleton fracture zone transform apparently is stepping eastward to join with a transform along the South Scotia Ridge.

majority of the teleseismic events between 1964 and 1992 are swarms of moderate-magnitude events which lasted up to six months (International Seismological Centre Earthquake Catalogs (ISC), 1964–1993).

The December 1967 eruption of Deception Island produced three teleseismic events, although two of them were mislocated almost 30 km from Deception Island. One event occurred in connection with the 1969 eruption. The 1970 eruption produced four events located at depths of 45 to 49 km, one event at 9 km with no magnitude determination, and one magnitude 4.6 event with no depth determination (ISC catalogue, 1970). Three swarms of five to eight events not associated with volcanic eruptions occurred near Deception Island in 1971, 1974, and 1982. In 1989 a single event at 10 km occurred near Deception Island (ISC catalogue, 1989). The events in 1971 and 1982, at 15 and 12 km, respectively, produced normal fault plane solutions indicative of extension (Pelayo and Wiens, 1989).

A large swarm of 24 separate events (magnitude 4.5 to 5.3) occurred near Bridgeman Island in the first six months of 1975. Nearly all the events were assigned depths of 33 km or less, except for one at 167 km. [This event was undoubtedly mislocated depthwise because of its low magnitude, 4.5, and the few stations which recorded it. Pelayo and Wiens (1989) do not show any events at such a depth.] One event near Bridgeman Island was recorded in 1990 at a depth of 10 km. These earthquakes may be related to ongoing extension rather than volcanic activity, because there is no historical evidence for volcanic activity on Bridgeman Island.

Elsewhere in Bransfield Strait two events relocated by Pelayo and Wiens (1989) lie at depths of 35 and 55 km (their events 10 and 18). Event 10 (61.4°S, 56.4°W) was a normal faulting event that may be in the upper plate if the seismic refraction work of Guterch *et al.* (1991) is correct. Event 18 (63°S, 61.9°W) at 55 km must be in the subducted slab although the Harvard catalogue, for that event lists its depth as 42 km. It is located almost directly on strike with the onshore projection of the Hero fracture zone, and may in fact be evidence of tearing along the subducted fracture zone.

In addition to the teleseismic events mentioned, a local network on Deception Island has operated for two months each austral summer since 1986 (Vila *et al.*, 1992). It has consistently recorded 1000 events per month with a total released seismic energy of about 3.0×10^{13} ergs/day. These events seem to be aligned parallel to the main fault system which crosses the island (E-W), and they follow the regional tectonic trend of the Bransfield rift (Vila *et al.*, 1992). The 1986–1992 events were grouped into two depth ranges, those from 0 to 2.5 km and those from 2.5 to 7.0 km. During the 1992–1993 austral summer this same network recorded five deep (55–85 km) events of magnitude 1.6–2.4 (SEAN, 1993), but it is unclear how such a closely spaced network could resolve deep events of such low magnitude.

5. SEISMIC REFRACTION

Early seismic refraction work found an anomalously thick layer beneath Bransfield Strait with a seismic velocity lower than that of normal mantle material but higher than typical continental crust (Ashcroft, 1972). Later seismic refraction work in Bransfield Strait (Guterch *et al.*, 1985, 1991, 1992; Grad *et al.*, 1993) identified returns from the Moho that dips from 10 km in the South Shetland Trench to 40 km below the South Shetland Islands,

and also at 40 km below the Antarctic Peninsula. Grad *et al.* (1993) recorded a seismic boundary in the lower lithosphere that ranged in depth from 35 to 80 km as shown in Fig. 8.3. Both the Moho and the lower seismic boundary dip at an angle of 25°, which was interpreted to be the dip of the remnant Phoenix plate under the Antarctic plate. Although published gravity coverage is not extensive, Bouguer gravity anomalies (Renner *et al.*, 1985) of up to +100 mgal correlate with the anomalous crustal structure found by Grad *et al.* (1993) under the South Shetland Islands and Bransfield Strait.

The sequence stratigraphy of Bransfield Basin is discussed by Jeffers and Anderson (1990) and was used by Grad *et al.* (1993) to constrain their seismic velocity model. They found an anomalous layer under Bransfield Basin with seismic wave velocities of $v_p > 7.0$ km s^{-1}. Unfortunately this high-velocity layer obscures the normal Moho transition as seen under the South Shetland Islands and under the Antarctic Peninsula. This anomalous layer is overlain by layers with velocities of 2.5, 4.2, and 5.6 km s^{-1}. The upper layer consists of 0.2 to 1.0 km of unconsolidated to poorly consolidated young sediments with substantial amounts of lava and tuff. The second layer consists of 1.2 to 2.5 km of older and better consolidated sediments, lava, and tuff. In the 2- to 7-km depth range, Grad *et al.* (1993) found an approximately 10-km-wide body with velocity $v_p = 6.8$ km s^{-1}. They attribute this body to be the active Bransfield rift. The active rift is manifested in the basin itself as submarine volcanoes, intrusive dykes, large magnetic anomalies, and high heat flow.

6. SEISMIC REFLECTION

There are numerous multichannel seismic and single-channel seismic lines known to have been collected in Bransfield Strait, including ones done by the British Antarctic Survey (Larter, 1991; Barker *et al.*, 1992), German scientists as part of the GRAPE (*G*eophysical *R*esearch Group for the *A*ntarctic *PE*ninsula) Team (1990), Polish scientists (Guterch *et al.*, 1985), Brazilian scientists (Gambôa and Maldonado, 1990), Spanish scientists (Acosta *et al.*, 1992a,b), U.S. scientists (Lawver and Villinger, 1989; Nagihara and Lawver, 1989; Jeffers and Anderson, 1990; Jeffers *et al.*, 1991; Barker and Austin, 1994), and other presently unpublished work from Italian, Chinese, Japanese, and Korean cruises. Barker (1976) published the first seismic profile for Bransfield Strait, while Guterch *et al.* (1985) presented the first seismic reflection lines to demonstrate the "complex crustal structure in the trough of Bransfield Strait." Their profile crosses the southern end of the central Bransfield Basin and clearly shows a neovolcanic intrusion zone. Jeffers and Anderson (1990) published a number of line drawings of seismic reflection data from Bransfield Strait, including one line that nearly duplicated the earlier Polish line. They determined that the sedimentation is dominated by glacial-marine processes with associated lithofacies. The central basin has received terrigenous sediment from the Trinity Peninsula and from the South Shetland Islands (Jeffers and Anderson, 1990). They discuss basinward transport of sediment through deeply incised troughs that form a prograding complex of coalescing trough-sourced wedges, although when the troughs are not active, principally during interglacial periods, the supply of terrigenous sediment to the basin is relatively low and sedimentation is predominantly biogenic. Although they state that the volcanic ridge acts as a barrier to sediment transport across the basin, later bathymetric mapping of the basin revealed that the volcanic ridge is not continuous, so it would not act

as a complete barrier (Klepeis and Lawver, 1994). In places, the neovolcanic ridge is easily defined as a linear wall less than half a kilometer across with nearly sheer sides that are at least a few hundred meters high. It was recently dredged (Keller *et al.*, 1994) and produced fresh glassy basalts.

Gambôa and Maldonado (1990) presented multichannel seismic reflection data collected in 1987 and 1988 by the Brazilian Antarctic Program. In each of their crossings they show a "spreading center" and ponded turbidites. On all multichannel seismic lines across Bransfield Strait, there is never more than 1 s of recent ponded turbiditic sediment. The GRAPE team (1990) published preliminary results from 1400 km of reflection seismic profiles from Bransfield Strait and the adjoining peninsula region. Their profile 9 crossed the major submarine volcano just off King George Island (also shown in Barker, 1976), and they identified an additional "magmatically influenced" zone just to the southeast of the volcanic edifice toward the Antarctic Peninsula. Larter (1991) questioned the designation of certain crust in Bransfield Strait as oceanic crust based solely on the reflection character of the top of acoustic basement, as the GRAPE team (1990) did. The unusual thickness of the crust found from the seismic refraction data would also suggest a lack of true oceanic crust.

Acosta *et al.* (1992b) present line drawings of single channel seismic reflection profiles that show the southeastern flank of the South Shetland Islands to be broken by faults into horsts and grabens which have been intruded by dikes and plugs. Barker and Austin (1994) display initial results of the R/V *Ewing* multichannel seismic reflection cruise, where they found complex fan-faulting patterns (Fig. 8.6) along the Antarctic Peninsula side of

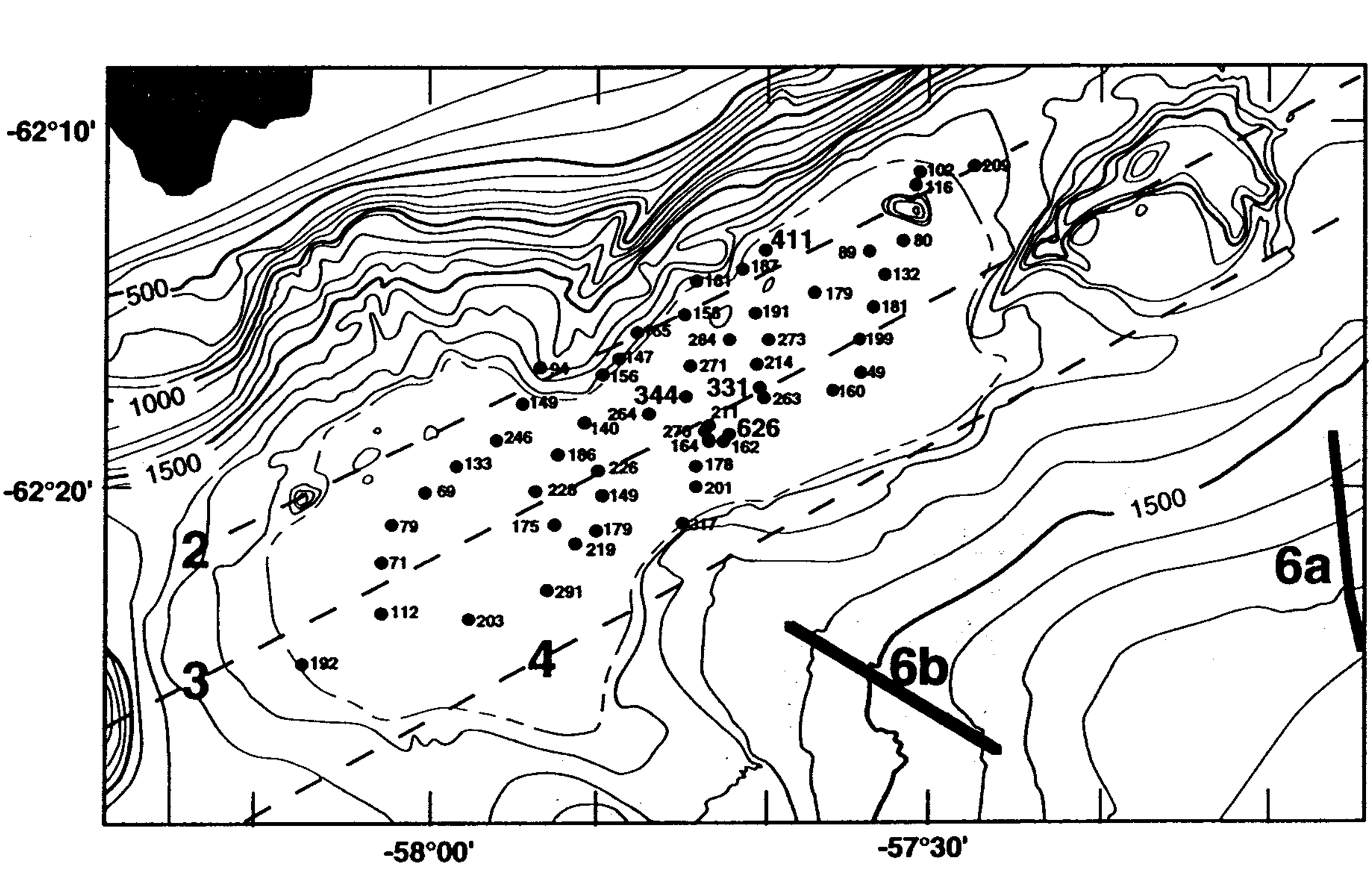

FIGURE 8.8. Heat flow map of the King George Basin. Heat flow in mW m^{-2}. Four highest values are shown with larger type size. Bathymetric contours are shown every 100 m with 500-m contours shown as bold lines. The inner, dashed, closed contour is the 1980-m contour showing the flat floor of the King George Basin that is uniformly between 1980 m and 2000 m with the exception of the linear volcanic mounds found along dashed line 2. Dashed lines labeled 2, 3, and 4 correspond to parallel volcanic lineations shown in Fig. 8.4. Thick lines labeled 6a and 6b are the locations of the seismic sections shown in Fig. 8.6. Shaded area is diapir zone of recent? activity taken from Barker and Austin (1994).

Bransfield Strait. They interpret the fanfaulting to be intracrustal diapirism that indicates a new zone of diffuse extension. They found a new zone of active extension on the margin of King George Basin toward the Peninsula from the four zones discussed above.

7. MAGNETICS

Aeromagnetic surveys of the Bransfield Strait region show a central positive anomaly along the axis of the deepest part of the strait (Garrett, 1990; Gonzalez-Ferran, 1991; Maslanyj *et al.*, 1991). This central high has been modeled as a large, positively magnetized igneous body associated with the inferred axis of rifting (Parra *et al.*, 1984; Gonzalez-Ferran, 1991). Gonzalez-Ferran (1991) concluded that reversely magnetized crust at the flanks of the central body best fit the data, and that a total of approximately 15 km of new crust has been created by 2 m.y. of spreading in Bransfield Strait.

Roach (1978) modeled detailed marine magnetic data from Bransfield Strait and found that only normally magnetized crust existed beneath the axial trough. Roach later reported (in Barker and Dalziel, 1983) that narrow strips of reversely magnetized crust were required at the margins of the axial trough, and a total of about 30 km of spreading had occurred since 1.3 Ma. Unfortunately his data and the details of his modeling were not published, although his results are now widely cited in the literature as evidence for a 1–2 Ma age for Bransfield Strait. Such a short magnetic anomaly profile is ambiguous, and models of it are poorly constrained. It may also be inaccurate to assume for the purpose of modeling that there is true seafloor spreading in Bransfield Strait, since seismic refraction data (see Section 5) suggest that the crust in Bransfield Strait is too thick to be normal oceanic crust. No spreading center has been identified, and the recent volcanism is dispersed along several lineaments in Bransfield Strait (Klepeis and Lawver, 1994). The thick sediment cover contains interbedded basalt flows and hides basement topography that affect the analyses of marine magnetic anomalies in the basin and complicate any modeling, as discussed by Lawver and Hawkins (1978).

8. HEAT FLOW

Heat flow measurements have been made in the King George Basin (Fig. 8.8) immediately south of King George Island. In the King George Basin the seafloor is flat (1.96 to 1.99 km), well sedimented, and covers an area of roughly 10 to 18 km by 45 km. Thermal gradients were measured at 63 locations, and *in situ* thermal conductivities were measured at 25 sites. The *in situ* conductivity matches thermal conductivity measurements made on piston core samples. The heat flow values range from 49 to 626 mW m^{-2} and are generally high, with about 25% of the values greater than 220 mW m^{-2}. There is significant local variation in values, with the highest values in the central part of the basin and along the southeast and northeast edges of the basin. In the western part of the basin values are generally less than 100 mW m^{-2}.

The highest value (626 mW m^{-2}) is near the center of the basin, although five additional measurements within a few hundred meters of this high value vary from 150 to 250 mW m^{-2}, typical of regions with active hydrothermal circulation. While this region of very high heat flow is not in line with the volcanic islands and submarine volcanoes of Bransfield rift, it is close to a region of recent faulting seen in the multichannel seismic

reflection data (Fig. 8.8). The second highest recorded heat flow value (411 mW m^{-2}) was found on the northeast edge of the basin in an area of mounds a few meters in height and up to a kilometer in diameter.

9. HYDROTHERMAL ACTIVITY

Evidence for hydrothermal activity in Bransfield Strait has been found in the water column and in the sediments. In the waters of Bransfield Strait, δ^3He increases from less than zero near the surface to >7 at depth. This has been interpreted as evidence for injection of ^{3}He into the water by backarc rifting (Schlosser *et al.*, 1988). Mn concentrations in the water also increase with depth to a maximum of almost 7 nM. Temperature changes are less pronounced, but appear to mimic the Mn profiles (Suess *et al.*, 1988). Maturation of biogenic components in the sediments (Whiticar *et al.*, 1985; Brault and Simoneit, 1990) is similar to the thermogenic hydrocarbons found to be associated with hydrothermal activity in the Gulf of California (Simoneit, 1983). Significant downcore decreases in amino acid abundances despite relatively constant δ^{13}C, δ^{15}N, C/N, and percent carbonate C in the sediments suggest hydrothermally accelerated complexation of amino acids (Silfer *et al.*, 1990).

Within the area of high and variable heat flow in King George Basin, several hundred grams of sediment were recovered in the heat flow probe. Qualitative analysis of this sediment by an electron microprobe indicated the presence of grains of Fe sulfide, Fe-Zn sulfide, Fe-Zn-Cu sulfide, Zn chloride, and metals or oxides of Zn and Fe, all presumed to be products of hydrothermal activity. This indicates hydrothermal activity occurred in the region of high heat flow (62°14′S, 57°44′W) and water-column measurements indicate that hydrothermal circulation is still active.

10. PETROLOGY AND GEOCHEMISTRY

10.1. Regional

Volcanism near the northern end of the Antarctic Peninsula can be divided into the main arc phase and a later phase associated with rifting of the peninsula (Bransfield Strait) and volcanism on the Weddell Sea side of the peninsula (James Ross Island Volcanic Group). Volcanism is presently active on both sides of the peninsula; however, the composition of the rocks on the two sides are chemically distinct (Fig. 8.9) and are also chemically distinct from the earlier arc volcanism.

10.1.1. Antarctic Peninsula Arc

Although the crust beneath the South Shetland Islands is assumed to be continental, actual basement rocks are unknown. According to Birkenmajer (1992), the basement of Bransfield Strait consists of continental-type crust modified by basic intrusions. The oldest exposed rocks are metasediments on Livingston Island (Fig. 8.4) and are thought to be between late Carboniferous and Triassic in age (Thomson, 1992). Similar rocks on the Antarctic Peninsula are between Permian and Cretaceous in age (Pankhurst, 1983). The

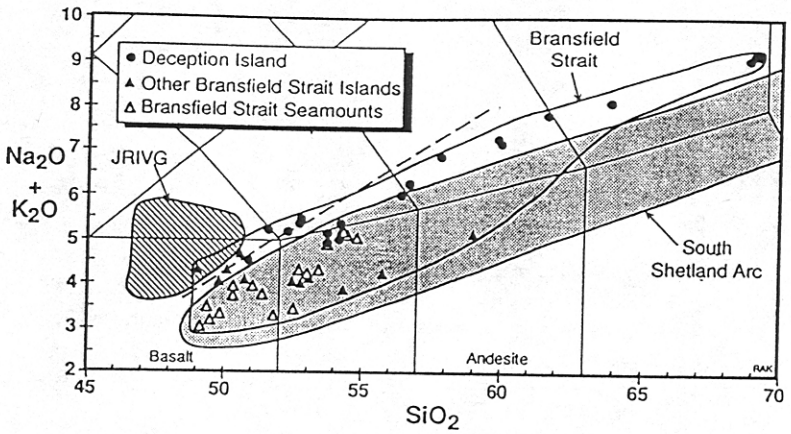

FIGURE 8.9. Weight percent SiO_2 versus weight percent Na_2O+K_2O for samples from the South Shetland island arc, Bransfield Strait, and the James Ross Island Volcanic Group (JRIVG). South Shetland arc data are from Saunders *et al.* (1980), Smellie (1988), Smellie *et al.* (1984, 1988), and Keller *et al.* (1992). Bransfield Strait data are from Keller and Fisk (1992) and Keller *et al.* (1992). Additional data from Bransfield Strait consistent with those shown here can be found in Weaver *et al.* (1979). JRIVG field is from data in Table III. Classification fields are from Le Bas *et al.* (1986). Dashed line is silica saturation line from Irvine and Baragar (1971).

oldest igneous rocks in the area are 155 to 185 Ma plutonic rocks on the northern Antarctic Peninsula near James Ross Island (Saunders *et al.*, 1982). K-Ar dates of 351 to 384 Ma of micas from granites from the same area have been reported (Rex, 1976) but are not confirmed by Rb-Sr dating. Plutonic rocks along the Bransfield Strait side of the peninsula are mostly 70 to 125 Ma, but some are as old as 130 to 145 Ma (Saunders *et al.*, 1982). The oldest extrusive rocks on the South Shetland Islands are late Jurassic–early Cretaceous volcaniclastic rocks on islands at the western end of the chain (Smellie *et al.*, 1980). A granodiorite intruding the volcaniclastic beds yielded a K-Ar age of 121 Ma (Smellie *et al.*, 1984). Additional isotopic ages suggest relatively continuous arc volcanism in the South Shetland Islands from late Jurassic to late Tertiary (Pankhurst and Smellie, 1983), although dates younger than about 20 Ma are extremely rare in the subduction-related volcanic rocks (Rex and Baker, 1973; Smellie *et al.*, 1984; Birkenmajer *et al.*, 1986).

Arc volcanism on the South Shetland Islands consisted mainly of calc-alkaline, high-alumina basalts, basaltic andesites, and low-silica andesites. Dacites and rhyolites are rare (Smellie, 1983; Smellie *et al.*, 1984). Exposures of intrusive rocks are less common and are mainly gabbros, tonalites, and granodiorites interpreted to be cogenetic with the extrusive rocks (Smellie, 1983). The chemistry and mineralogy of the pre-Quaternary South Shetland Islands have been described in detail by Smellie *et al.* (1984). Islands in the southern part of Bransfield Strait, close to the Antarctic Peninsula, are Eocene–Oligocene arc tholeiites similar to rocks on the South Shetland Islands (Rex, 1976; Baker *et al.*, 1977).

Pre-Quaternary volcanic arc rocks from the South Shetland Islands and northern Antarctic Peninsula are calc-alkaline with mild tholeiitic tendencies (Smellie *et al.*, 1984). Chemical variations within the arc magmas can be accounted for by fractional crystallization and slight differences in extent of partial melting of the source (Smellie, 1983). Their alkalinity (Fig. 8.9) and trace element abundances (Saunders *et al.*, 1980; Smellie *et al.*, 1984) are typical of island-arc rocks; that is, the large-ion lithophile elements (e.g., Rb, Ba, K, and Ce) are enriched relative to the high-field-strength elements (e.g., Zr, Ti, and Nb). Normalized multielement plots show an obvious Nb depletion (Fig. 8.10).

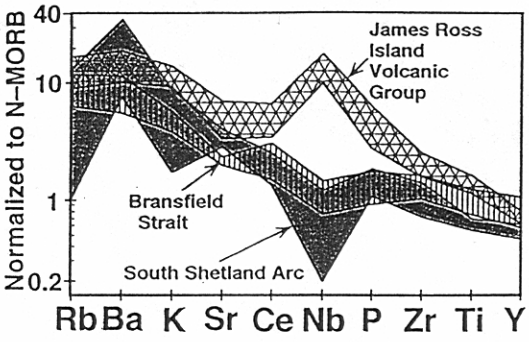

FIGURE 8.10. N-MORB-normalized multielement plot for basalts from the South Shetland arc (Tertiary basalts only), Bransfield Strait (seamounts only), and James Ross Island Volcanic Group. Data sources as in Fig. 8.9. N-MORB normalization values are from Saunders and Tarney (1984). Increasing distance from the South Shetland Trench corresponds to increasing Nb and decreasing Ba/Nb.

Strontium isotopic analyses are limited for the South Shetland Arc, but mainly range from 0.7033 to 0.7043 (Smellie *et al.*, 1984; Barbieri *et al.*, 1989; Jin Qingmin *et al.*, 1991; Keller *et al.*, 1992). The only Nd and Pb isotopic data available (excepting a single analysis in Keller *et al.*, 1992) are from the Fildes Peninsula on western King George Island and are published as ranges only: 0.51288 to 0.51301 for $^{143}Nd/^{144}Nd$, 18.503 to 18.641 for $^{206}Pb/^{204}Pb$, and 15.588 to 15.625 for $^{207}Pb/^{204}Pb$ (Jin Qingmin *et al.*, 1991). No $^{208}Pb/^{204}Pb$ data were included in Jin Qingmin *et al.* (1991). A single South Shetland arc basalt from the Low Head area of King George Island had $^{87}Sr/^{86}Sr$, $^{143}Nd/^{144}Nd$, and $^{207}Pb/^{204}Pb$ within the ranges reported by Jin Qingmin *et al.* (1991) but had higher $^{206}Pb/^{204}Pb$ (Keller *et al.*, 1992).

10.1.2. Bransfield Strait

Quaternary volcanism in Bransfield Strait occurred on Deception, Penguin, and Bridgeman Islands (Weaver *et al.*, 1979), and at a few isolated locations on King George, Livingston, and Greenwich Islands (Smellie, 1990), and on seamounts and ridges between Deception and Bridgeman Islands (Fig. 8.4; Fisk, 1990; Keller *et al.*, 1994). All reported K-Ar dates from the Bransfield Strait islands and seamounts are 300 ka or less (Table I). Deception Island is historically active (e.g., Smellie, 1990), and the most recent volcanism on Penguin Island was probably within the last 300 years (Birkenmajer, 1980). All of the sampled seamounts yielded fresh, glassy basalts (Fisk, 1990; Keller *et al.*, 1994).

The Quaternary volcanic centers in Bransfield Strait are mainly olivine basalts and basaltic andesites, although Deception Island erupted a complete basalt-to-trachydacite evolutionary suite (Keller *et al.*, 1992). Bridgeman Island is composed of basaltic andesites, while Melville Peak and Penguin Island are olivine basalts and scoria (Weaver *et al.*, 1979; Keller *et al.*, 1992). The seamounts are aphyric to olivine-plagioclase-phyric, vesicular, tholeiitic basalts, and basaltic andesites (Fig. 8.9; Fisk, 1990; Keller and Fisk, 1992).

The Bransfield Strait samples, with the exceptions of the sodic samples from Penguin and Deception Islands, can be classified as subalkaline basalts and basaltic andesites (Table II). They all have higher concentrations of the alkali and alkali earth elements (e.g., Na, K, Rb, Sr, and Ba), and less of an Fe enrichment trend than typical mid-ocean ridge tholeiites (Fisk, 1990; Keller *et al.*, 1992). Many of the Quaternary basalts are similar to the older-arc rocks in silica versus total alkalies (Fig. 8.9). Trace element concentrations are slightly to moderately enriched relative to N-MORB, and show a subtle negative Nb anomaly when normalized to N-MORB (Fig. 8.10). Low-pressure, fractional crystallization of olivine, spinel, and plagioclase can account for the chemical variation between samples from an individual volcano (Keller and Fisk, 1992; Keller *et al.*, 1992). Sr-isotopic ratios

TABLE I
K-Ar Data for Basalts from Bransfield Strait and the James Ross Island Volcanic Group

Location	Sample	K (wt%)	$^{40}Ar_{rad}$ (10^{-9} cc/g)	$^{40}Ar_{rad}$ (%)	Age ± 1 σ (10^3 yr)	Ref.[a]
Bransfield Strait						
King George Island						
Melville Peak	MP372	0.694	6.229	6.7	231 ± 19	3
Melville Peak	MP375	0.767	2.137	2.2	72 ± 15	3
Melville Peak	MP406	0.802	9.240	5.3	296 ± 27	3
Livingston Island						
Gleaner Heights	P.51.1	0.433	0.001	0.2	100 ± 400	4
Greenwich Island						
Mt. Plymouth	P.54.1	0.305	0.002	0.4	200 ± 300	4
Mt. Plymouth	P.55.1	0.300	0.002	0.5	200 ± 400	4
Deception Island	D1048	0.390	2.266	0.928	105 ± 46	1
Bridgeman Island	B2	0.581	1.414	0.932	63 ± 25	1
Eastern Seamount	300.13	0.435	0.8779	0.2744	53 ± 36	2
Western Seamount	310.14	0.418	1.631	0.6808	103 ± 35	2
James Ross Island Volcanic Group						
James Ross Island, Prince Gustav Channel islands, Vega Island, Humps Island, and Paulet Island				300 ± 100 to 7130 ± 490		5,6
James Ross Island						
Dreadnought	4M18	0.838	216.6	26.3	6643 ± 102	1
Villar Fabre	5M117	1.063	162.9	13.7	3940 ± 85	1
Cockburn Island	CK3	0.992	129.7	31.3	2781 ± 32	1

[a]Reference codes: 1—This paper; 2—Fisk (1990); 3—Birkenmajer and Keller (1990); 4—Smellie et al. (1984); 5—Smellie *et al.* (1988); 6—Sykes (1988). Samples with reference codes 1, 2, and 3 were analyzed at Oregon State University using techniques described in Fisk (1990).

range from 0.70304 to 0.70386, and Nd-isotopic ratios from 0.51287 to 0.51301. Pb isotopes range from 18.691 to 18.757 ($^{206}Pb/^{204}Pb$), 15.594 to 15.624 ($^{207}Pb/^{204}Pb$), and 38.441 to 38.556 ($^{208}Pb/^{204}Pb$) (Keller *et al.*, 1992).

10.1.3. James Ross Island Volcanic Group

The James Ross Island Volcanic Group (JRIVG) crops out on the northern tip of the Antarctic Peninsula and on numerous islands in the northwestern Weddell Sea in a backarc setting that may be analogous to the Patagonia Plateau basalts. Many outcrops of the JRIVG are sheer cliffs of palagonitized basaltic hyaloclastite and pillow breccia capped by coeval basalt flows (Nelson, 1966). Basaltic dikes intrude the underlying Cretaceous sediments and Tertiary glacial deposits. The basalts are mainly alkalic (Fig. 8.9), but hypersthene- and quartz-normative tholeiites have also been reported (Smellie, 1987). The oldest rocks in the JRIVG are 7 Ma basalt clasts in glacial deposits beneath the main volcanic pile on James Ross Island (Table I). Volcanic activity continued through the Pliocene and Quaternary, with the youngest K-Ar date being less than 0.3 Ma (Table I). The most recent activity on James Ross Island occurred at three volcanic cones near the margin of the ice cap. These cones are undisrupted by glacial activity and are undoubtedly of a very young age (Strelin *et al.*, 1993).

The alkalic basalts of the JRIVG are chemically distinct from both the South Shetland

TABLE II

Representative Whole Rock Major and Trace Element Concentration for Quaternary Volcanic Rocks from Bransfield Strait[a]

	Western seamount		Eastern seamount		Axial ridge	Deception Island						Bridgeman Island	Penguin Island	Melville Peak
Sample	292.18	310.07	297.01	309.01	DF86.32	D1048	D1082	D1051	D1055	D1075	D1060	B1	P174	MP405
SiO_2	49.5	50.4	52.5	54.3	54.3	50.9	53.8	51.6	68.9	63.9	57.8	55.8	50.6	52.8
TiO_2	1.13	1.54	1.05	1.71	1.82	1.58	1.82	2.44	0.60	1.12	1.86	0.78	1.30	0.92
Al_2O_3	14.1	16.3	16.9	15.7	15.8	17.3	16.2	15.2	14.5	15.6	15.6	18.7	17.2	16.7
FeO*	8.6	9.0	7.1	10.1	9.6	8.4	9.0	11.0	4.3	6.7	8.6	6.6	8.7	7.1
MnO	0.16	0.16	0.14	0.17	0.19	0.15	0.17	0.19	0.15	0.17	0.17	0.12	0.16	0.14
MgO	12.3	6.7	7.0	3.7	4.4	6.1	4.6	4.9	0.3	1.2	2.6	5.0	7.9	7.1
CaO	10.4	10.9	11.3	7.4	8.1	10.3	8.9	9.1	1.8	3.6	6.0	9.4	10.2	11.3
Na_2O	2.73	3.40	3.04	4.23	4.72	4.05	4.40	4.71	7.17	6.67	5.90	3.52	3.99	3.09
K_20	0.46	0.55	0.39	0.97	0.45	0.47	0.51	0.50	1.89	1.43	0.96	0.70	0.66	0.91
P_2O_5	0.16	0.19	0.12	0.23	0.30	0.25	0.29	0.36	0.12	0.42	0.37	0.08	0.29	0.14
Total	99.56	99.08	99.56	98.49	99.65	99.55	99.66	100.06	99.71	100.76	99.77	100.64	100.96	100.16
Sc	35	32	31	30	27	32	35	37	11	17	20	29	29	42
V	256	328	220	351	235	245	265	336	13	50	194	210	282	249
Cr	618	192	228	8	23	106	42	44	0	2	9	40	218	157
Ni	283	80	84	3	8	28	14	14	9	7	1	27	95	41
Cu	68	76	54	70	29	31	30	47	8	17	54	92	154	79
Zn	63	69	56	92	85	66	77	81	87	90	85	56	71	55
Ga	16	19	16	17	21	17	19	21	24	23	20	17	22	18
Rb	10	10	7	17	4	7	9	5	30	21	14	17	7	17
Sr	255	266	280	330	189	465	374	350	130	254	325	357	636	598
Y	23	26	21	37	52	26	33	36	62	56	43	14	16	21
Zr	93	104	94	154	197	143	167	171	444	355	249	72	90	112
Nb	2	4	2	4	7	7	7	8	16	14	10	1	2	2
Ba	91	98	65	144	6	40	62	29	256	167	130	76	146	173
Zr/Y	4.0	4.0	4.5	4.2	3.8	5.5	5.1	4.8	7.2	6.3	5.8	5.1	5.6	5.3

[a]Concentrations were determined by x-ray fluorescence at Washington State University, and are given as weight percent oxides for the major elements and parts per million for the trace elements. FeO* is total Fe as FeO. Data for Western and Eastern seamounts are from Keller and Fisk (1992). Other data are from Keller *et al.* (1992). Data for Deception, Bridgeman, and Penguin Islands and Melville Peak have also been published by other workers (e.g., Weaver *et al.*, 1982; Smellie, 1990) and are comparable to data given here.

arc and from the <1 Ma Bransfield Strait basalts. The JRIVG tends to have lower SiO_2 (Fig. 8.9), and higher K_2O and TiO_2 (Table III). Paulet Island, especially, is high in total alkalies, Al_2O_3, and many incompatible trace elements. High concentrations of alkalies and incompatible trace elements in the JRIVG are reminiscent of many continental-rift basalts and alkalic ocean island basalts. Their prominent Nb hump on the MORB-normalized multi-element plot (Fig. 8.10) is a common characteristic of intraplate basalts not associated with a subduction zone and is in marked contrast to the Nb depletions of the South Shetland arc and Bransfield Strait backarc basalts. The $^{87}Sr/^{86}Sr$ values range from 0.70306 to 0.70348, and $^{143}Nd/^{144}Nd$ from 0.51282 to 0.51293 (Keller *et al.*, 1993), which places them in the lower left quadrant in $^{87}Sr/^{86}Sr$ versus $^{143}Nd/^{144}Nd$ space, displaced toward St. Helena–type values.

10.1.4. Temporal Comparison

The hiatus between the end of arc volcanism on the South Shetland Islands and the beginning of volcanism in Bransfield Strait was approximately 20 m.y., but the major and trace element compositions are similar in some cases (Figs. 8.9 and 8.10). Bridgeman Island, in particular, could be mistaken for an island-arc tholeiite (Table II). The submarine samples, on the other hand, are more similar to backarc basin basalt (i.e., a hybrid of arc and mid-ocean ridge basalt compositions; Fisk, 1990). The isotopic ratios of the arc and backarc rocks are also similar, which implies that they all were derived from similar sources. However, the lack of trace element and isotopic data from the South Shetland Islands and the lack of samples from Bransfield Strait (partially rectified in 1993) preclude thorough comparisons.

10.1.5. Across-Arc Comparison

The importance of the chemical contribution from a subducting slab has been shown to decrease with distance from the trench in southern South America (Stern *et al.*, 1990). On the northern Antarctic Peninsula, the occurrence of volcanism at a variety of distances from the South Shetland Trench (50–125 km for the South Shetland arc, 125–150 km for the Bransfield Strait, and 300–400 km for the James Ross Island Volcanic Group) is an excellent chance to constrain the spatial extent of contamination of the mantle by a subducting slab. On the northern Antarctic Peninsula we see an obvious decrease in contribution from the subducted slab with increasing distance from the trench. The high Ba and low Nb of the South Shetland arc samples are typical of the subduction-zone influence found in many volcanic arcs. The Bransfield Strait basalts are farther from the trench, have a slight negative Nb anomaly, and are moderately enriched in the alkalies relative to MORB. This is typical of backarc basin basalts, and suggests less of a contribution from the subducted slab. The JRIVG basalts are farthest from the South Shetland Trench and do not show any evidence for the influence of the slab subducting at the trench. Their high Nb is typical of intraplate basalts and is the opposite of what would be expected if their source had been contaminated by subduction (Keller *et al.*, 1993). Apparently, between 150 and 300 km is the greatest distance that the subducting slab can influence the chemistry of the volcanism above it.

Some published comparisons of arc and backarc basalts suggest that the upwelling mantle in backarc regions contains an ocean island basalt (OIB) component (Stern *et al.*, 1990; Hickey-Vargas, 1992). This OIB component can be seen in the JRIVG data but not

TABLE III

James Ross Island Volcanic Group Whole Rock Major and Trace Element Concentrations by X-ray Fluorescence[a]

	James Ross Island																
	Hidden Lake		Dreadnought		Massey				Conico	Ventisca	Kotick		Villar Fabre				
Lat (S)	64°02′		64°00′		63°57′				63°56′	63°57′	64°01′		64°06′				
Lon (W)	58°18′		57°50′		57°58′				58°08′	58°04′	58°22′		58°22′				
SiO_2	48.1	47.9	48.5	48.2	50.2	47.1	47.4	48.5	50.4	47.1	46.8	48.4	48.3	48.4	47.9	49.8	48.2
TiO_2	1.78	2.01	2.09	1.89	1.84	1.71	1.95	2.04	1.87	1.71	1.75	1.55	1.69	1.59	1.64	1.77	1.74
Al_2O_3	15.1	16.1	16.0	15.7	16.4	15.4	15.7	16.1	16.3	15.1	15.1	14.9	15.3	15.5	15.0	15.8	15.1
FeO*	10.5	10.0	9.8	10.4	9.5	10.9	10.2	10.6	9.7	10.7	10.5	10.9	10.6	10.8	11.1	10.4	12.0
MnO	0.16	0.17	0.16	0.16	0.15	0.17	0.16	0.17	0.16	0.16	0.16	0.17	0.15	0.16	0.17	0.15	0.18
MgO	8.9	7.2	7.6	7.9	6.7	8.1	8.6	8.4	6.8	10.3	10.0	9.2	9.1	8.9	8.6	7.8	9.1
CaO	8.2	9.9	8.9	9.2	8.3	8.4	8.4	9.5	9.2	8.0	8.5	8.6	8.0	7.9	7.8	7.9	8.0
Na_2O	3.34	3.56	3.39	3.37	3.83	3.34	3.64	3.57	3.58	2.58	2.96	3.11	3.27	3.16	3.43	3.71	3.27
K_2O	1.20	0.93	1.13	1.01	1.59	0.83	1.44	1.19	1.37	1.13	0.89	0.72	1.01	0.92	1.05	1.28	0.95
P_2O_5	0.38	0.38	0.47	0.49	0.49	0.35	0.63	0.50	0.36	0.42	0.33	0.28	0.38	0.36	0.37	0.54	0.21
Total	97.57	98.16	98.10	98.38	98.96	96.17	97.99	100.55	99.71	97.15	96.94	97.73	97.64	97.66	97.02	99.17	98.72
Sc	19	27	28	27	23	24	22	29	30	20	26	20	22	21	19	13	25
V	176	207	191	180	169	159	169	197	195	149	167	166	146	154	151	150	148
Cr	276	178	207	256	188	223	228	239	184	313	304	272	233	231	226	199	225
Ni	166	75	94	115	96	146	157	116	86	200	180	180	177	162	168	145	170
Cu	41	39	48	50	37	58	56	49	44	48	42	52	44	51	41	47	35
Zn	92	83	85	82	90	93	87	81	87	88	90	90	101	99	99	97	90
Ga	16	17	19	15	17	16	18	15	19	21	16	18	18	18	15	17	20
Rb	17	11	13	12	19	10	17	13	25	10	13	11	10	9	13	12	10
Sr	506	510	607	611	701	453	742	618	481	686	510	359	482	446	475	653	395
Y	24	25	24	26	24	24	25	26	28	22	22	25	24	22	24	21	19
Zr	154	168	191	178	203	162	226	180	164	174	134	129	142	141	142	197	139
Nb	27	29	36	40	41	38	41	39	28	28	24	17	24	25	24	38	23

	James Ross Island												Paulet Island				Cockburn Island	
	Sta Marta	Dobson			Ekelof	Coley	Marina			Elba								
Lat (S)	63°54′	64°02′			64°12′	64°11′	64°10′			64°15′			63°35′				64°12′	
Lon (W)	57°54′	57°56′			57°14′	57°10′	57°22′			57°30′			55°46′				56°54′	
SiO_2	47.2	48.0	47.8	48.3	46.1	48.3	48.9	48.5	48.8	48.7	48.8	48.5	48.2	47.4	46.9	47.8	48.0	48.8
TiO_2	1.73	1.56	1.65	1.64	2.12	2.11	1.99	2.00	1.95	2.44	2.45	2.46	2.26	2.26	2.26	2.30	1.82	1.86
Al_2O_3	15.4	15.5	15.2	15.4	14.6	15.7	15.4	15.3	15.3	18.2	18.4	18.3	16.9	16.9	16.7	17.0	16.0	16.4
FeO*	10.3	10.9	10.6	11.0	10.9	10.7	10.4	10.4	10.2	10.4	10.2	10.8	9.7	9.6	9.5	9.3	10.5	10.3
MnO	0.17	0.17	0.17	0.17	0.16	0.16	0.16	0.16	0.15	0.16	0.16	0.16	0.16	0.16	0.16	0.16	0.16	0.16
MgO	8.5	9.5	9.3	8.7	9.4	7.6	8.9	9.0	8.9	4.7	4.8	4.6	7.7	6.6	6.9	6.7	7.0	6.7
CaO	7.8	8.7	8.7	8.6	8.2	9.5	8.0	7.9	7.8	7.6	7.4	7.3	9.3	8.9	9.1	9.2	8.6	8.7
Na_2O	3.74	3.11	3.27	3.37	4.03	3.50	4.10	3.99	4.35	4.89	5.32	4.93	4.21	4.16	4.30	4.33	3.69	3.59
K_2O	1.38	0.82	0.91	0.88	1.17	1.05	1.57	1.56	1.65	1.55	1.97	1.82	1.40	1.43	1.37	1.44	1.16	1.22
P_2O_5	0.52	0.32	0.37	0.36	0.96	0.38	0.63	0.62	0.64	0.75	0.84	0.84	0.81	0.75	0.75	0.86	0.40	0.43
Total	96.79	98.54	98.02	98.56	97.63	98.97	99.96	99.48	99.66	99.29	100.24	99.72	100.68	98.19	97.83	99.03	97.27	97.99
Sc	17	30	27	23	18	26	23	22	21	16	17	18	28	23	23	22	24	25
V	151	185	195	189	137	211	165	177	185	126	151	121	185	187	204	191	173	177
Cr	237	295	294	260	288	224	288	288	282	10	10	10	180	102	114	115	180	150
Ni	191	189	188	164	206	86	132	138	135	12	17	17	99	69	78	74	96	77
Cu	47	53	59	61	47	21	29	34	29	29	27	21	29	31	41	43	19	29
Zn	92	85	87	88	98	90	93	87	91	78	82	86	74	75	81	75	85	81
Ga	17	17	17	18	15	21	21	20	19	18	18	22	19	19	16	20	18	20
Rb	11	13	13	15	11	11	17	17	17	13	17	16	17	17	16	16	16	16
Sr	593	435	431	433	1383	536	728	720	732	945	911	917	951	940	943	937	536	547
Y	22	22	25	25	21	25	23	23	23	29	28	29	28	30	29	28	23	25
Zr	179	120	131	135	296	149	206	205	208	254	250	254	225	229	216	228	163	170
Nb	34	19	21	24	91	26	43	43	43	55	55	55	45	47	46	48	26	27

[a]Concentrations were determined by x-ray fluorescence at Washington State University using techniques described in Keller *et al.* (1992), and are given as weight percent oxides for the major elements and parts per million for the trace elements. FeO* is total Fe as FeO. Data for Paulet Island and some of these locations on James Ross Island have also been published by other workers (Nelson, 1966; Baker *et al.*, 1977; Smellie, 1987) and are comparable to the data given here.

in the Bransfield Strait data (Keller *et al.*, 1992). Apparently the OIB component is not available or is not melted beneath Bransfield Strait, just as the subducted component does not appear in the JRIVG lavas. The presence of a subducted slab beneath James Ross Island should rule out the possibility that a rising plume or hot spot is responsible for the OIB-like compositions of the JRIVG. Also, the "slab-window" hypothesis that has been suggested for the origin of similar alkalic basalts found farther south on the Antarctic Peninsula at Seal Nunataks and Alexander Island (Hole *et al.*, 1991) cannot apply to James Ross Island.

10.2. Intra-Bransfield Strait Comparison

All of the recent (≤300 ka) episode of volcanic activity in Bransfield Strait can be classified as basalts to basaltic andesites, and on Deception Island as basalts to dacites. These rocks appear to be the product of <5% to 15% melting of mantle that contained 0.5% to 2% of a subducted component (Keller *et al.*, 1992). Within these rocks, however, we identify three contrasts in chemistry that are correlated with differences in mode or location of eruption: (1) on-axis versus off-axis, (2) submarine versus subaerial, and (3) northeast of 57°50′W versus southwest of 57°50′W. These differences are probably the result of different mantle sources and processes.

10.2.1. On Axis versus off Axis

The two off-axis volcanoes, Penguin Island and Melville Peak (Fig. 8.4), have high Sr, Ba, and K, and low Y relative to the on-axis basalts. Off-axis volcanic remnants on Livingston and Greenwich islands, possibly contemporary with Penguin Island and Melville Peak, also have high Sr and Ba and low Y, similar to Penguin Island and Melville Peak (Smellie *et al.*, 1984). The high-Sr abundances of Penguin Island and Melville Peak are not the result of crustal assimilation because other chemical changes that would be associated with this assimilation are not observed (Keller *et al.*, 1992). High Sr is also typical of the older (>20 Ma) volcanic arc rocks of the South Shetland Islands, so the off-axis Bransfield Strait volcanoes may have tapped the older arc mantle source. The lower $^{206}Pb/^{204}Pb$ of the off-axis samples also shows that the mantle that produced the off-axis lavas was chemically different from that which produced the on-axis basalts. The high Sr of Penguin Island and Melville Peak excludes the possibility of residual plagioclase in the mantle source (Keller *et al.*, 1992). Small amounts of melting of a deeper, mineralogically different (garnet-bearing) source is also suggested by the higher Ce/Sm (Keller *et al.*, 1992) and other trace elements (Weaver *et al.*, 1979) of the off-axis basalts. Thus, off-axis volcanoes appear to be the result of a smaller degree of melting of a deeper and chemically distinct mantle than on-axis volcanoes (Weaver *et al.*, 1979; Keller *et al.*, 1992).

10.2.2. Submarine versus Subaerial

The seamounts have lower Zr/Y ratios (~4; Table II) than the subaerial volcanoes (mostly >5). This difference is not a result of alteration, since both Zr and Y are relatively immobile during weathering and most of the rocks are fresh. The degree of melting of the mantle can affect the Zr/Y ratio; however, this effect is only significant for small (<5%) amounts of melt, which would also be expressed in much larger amounts of incompatible elements in the subaerial volcanoes than in the submarine ones. Some trace elements

(Ba, Rb, K), however, are lower in the subaerial volcanoes than in the submarine volcanoes, indicating that chemical differences between these two groups are not related to the degree of melting.

Most of the subaerial volcanoes are larger than the submarine volcanoes, so their higher Zr/Y may represent a characteristic of a volcano as it grows; that is, continuous partial melting of the mantle beneath the larger volcanoes could produce high Zr/Y, and the smaller submarine volcanoes have not yet evolved to this chemistry. Alternatively, the lower Zr/Y of the submarine basalts (which are closer to MORB values of 2.5 to 3.5) may indicate that as the rift develops and deepens, the volcanoes become MORB-like. The rift sample (DF86.32 in Table II) has the lowest Zr/Y (3.8) of any Bransfield Strait rock and appears to be the most similar to MORB. It also has the lowest Rb, Sr, and Ba. Finally, the larger volcanoes, which are mainly subaerial, may represent melting of deeper mantle where garnet is present.

10.2.3. Along Axis

The chemistry of basalts from backarc rifts can vary significantly along strike of the rift, as has been found in the Mariana Trough, Lau Basin, and Gulf of California (Saunders and Tarney, 1984; Hawkins and Melchior, 1985; and Hawkins *et al.*, 1990). This is also true of Bransfield Strait, where Na_2O increases and Rb/Sr decreases abruptly from NE to SW at approximately 57°50′W. The change occurs between Melville Peak and Penguin Island and is evident in all of the analyzed submarine and subaerial samples. Basalts that are northeast of this boundary also have lower total alkalies and lower $^{87}Sr/^{86}Sr$ at the same $^{143}Nd/^{144}Nd$ compared with basalts southwest of this boundary. The chemical boundary is found in the same general region as the highest heat flow.

The abrupt change in isotopes along axis indicates there is a change in mantle sources across the boundary, perhaps due to a change in age or composition of the subducted oceanic crust. The boundary approximately coincides with the onshore extrapolation of fracture zone E (Fig. 8.4), which separates younger crust to the southwest and older crust to the northeast (Larter and Barker, 1991). Alternatively, the chemical boundary may reflect the contrast between subducted oceanic crust created at the Antarctic–Phoenix Ridge versus oceanic crust created at the Nazca–Phoenix Ridge. Different inputs to the mantle wedge from the subducted slab could account for the isotopic differences as well as induce changes in melting or mineralogy in the mantle. Elsewhere, along-arc variations in basalt chemistry have been attributed to variations in the composition of the subducted material (e.g., Lin *et al.*, 1990).

11. CONCLUSIONS

Regional tectonics of the Antarctic Peninsula support the hypothesis that little or no active subduction is occurring beneath Bransfield Strait and the South Shetland Islands. What little subduction that may be occurring would be equal to the amount of extension in Bransfield Strait. Spreading ceased on the Antarctic–Phoenix spreading center at approximately 4 Ma. The remnant of the Phoenix plate was pinned under the South Shetland Islands, where it has been imaged to a depth of 40 km by seismic refraction results (Grad *et al.*, 1993). Teleseismic earthquakes do not indicate any motion of a subducted slab

beneath Bransfield Strait, although one event (event 18; Pelayo and Wiens, 1989) may have been produced along the downdip extension of the Hero fracture zone. Plate reorganization since ~4 Ma resulted in a 110° bend in the Antarctic–Scotia plate boundary that seems to have imposed extensional stress on the Bransfield Strait region.

Bransfield Strait is a region of recent extension based on active and recent volcanism, high heat flow, earthquake fault plane solutions, and seismic reflection data. This extension may also be associated with trench rollback at the South Shetland Trench and defines the SE boundary of the South Shetland Islands microplate. Seismic refraction results (Grad *et al.*, 1993) indicate that the crust under Bransfield Strait is anomalously thick, up to 30 km, with an unusual layer of crustal material with $v_p > 7.0$ km s^{-1}. They also found a 10-km-wide body with seismic velocity $v_p = 6.8$ km s^{-1}, which they interpreted to be the active Bransfield rift. Fault plane solutions (Pelayo and Wiens, 1989) from the Bransfield Strait region support active extension, and some earthquake swarms can be directly correlated to episodes of active volcanism. Barker and Austin (1994) and Lawver and Villinger (1989) show evidence of active crustal extension from seismic reflection results, supportive of continental crustal extension rather than normal seafloor spreading.

Active arc volcanism seems to have ceased at about 20 Ma. Recent Bransfield Strait basalts are chemically transitional between island-arc and ocean ridge basalts, a feature they share with many marginal basin basalts. Such chemistry agrees with the transitional nature of the tectonics of the strait (i.e., transitional between arc and spreading regimes). Considerable data supporting the existence of hydrothermal activity in Bransfield Strait have already been published. The new discovery of sulfide minerals in the sediments at a high heat flow site in Bransfield Strait is additional support for recent hydrothermal activity.

Acknowledgments

This work was supported by a number of National Science Foundation grants to the authors and to those that have provided us with their results. Grants include, but are not limited to, DPP-8916436 and DPP-9019247 to L. Lawver and DPP-8817126 to M. Fisk. Field work on James Ross Island was supported by the Argentine Antarctic Institute and Oregon State University. We are grateful to S. Porebski for donating the Cockburn Island samples, and to E. Godoy for donating the Paulet Island samples. GPS-navigated multi-beam bathymetry were collected on cruise 91-01 of R/V *Maurice Ewing* and two cruises of NOAA ship *Surveyor*. Heat flow data was collected on R/V *Polar Duke* cruise PD89-IV. We wish to thank the captains and crews from all those ships, without whose assistance this work would not have been possible. We would particularly like to thank Rob Larter, Dallas Abbott, and Daniel Barker for reviewing an unacceptably rough draft of this manuscript. This is UTIG contribution number 1062.

REFERENCES

Acosta, J., Herranz, P., and Sanz, J. L. 1992a. Perfiles sismicos en el rift de Bransfield, Campaña Exantarte 90/91, in *Geologica de la Antártida Occidental* (J. López-Martinez, ed.), pp. 195–202, Simposios T 3, III Congreso Geológico de España y VIII Congreso Latinoamericano de Geologia, Salamanca.

Acosta, J., Herranz, P., Sanz, J. L., and Uchupi, E. 1992b. Antarctic continental margin: Geological image of the

Bransfield Trough, an incipient oceanic basin, in *Geological Evolution of Atlantic Continental Rises* (C. W. Poag and P. C. Graciansky, eds.), pp. 49–61, Van Nostrand Reinhold, New York.

Anderson, J. A., Pope, P. G., and Thomas, M. A. 1990. Evolution and hydrocarbon potential of the northern Antarctica Peninsula continental shelf, in *Antarctica as an Exploration Frontier: Hydrocarbon Potential, Geology and Hazards* (B. St. John, ed.), pp. 1–12, Am. Assoc. Petrol. Geol., Studies in Geology 31.

Ashcroft, W. A. 1972. Crustal structure of the South Shetland Islands and Bransfield Strait, *Br. Antarc. Surv. Sci. Rep.* **66**.

Baker, P. E., Buckley, F., and Rex, D. C. 1977. Cenozoic volcanism in the Antarctic, *Phil. Trans. R. Soc. London* **279**:131–142.

Barbieri, M., Birkenmajer, K., Delitala, M. C., Francalanci, L., Narebski, W., Nicoletti, M., Peccerillo, A., Petrucciani, C., Todaro, M. L., Tolomeo, L., and Trudu, C. 1989. Preliminary petrological, geochemical and Sr isotopic investigation on Mesozoic to Cainozoic magmatism of King George Island, South Shetland Islands (West Antarctica), *Mineral. Petrogr. Acta (Bologna)* **32**:37–49.

Barker, D. H. N., and Austin, J.A., Jr. 1994. Crustal diapirism in Bransfield Strait, West Antarctica—evidence for distributed extension in marginal basin formation, *Geology* **22**:657–660.

Barker, P. F. 1976. The tectonic framework of Cenozoic volcanism in the Scotia Sea region, a review, in *Andean and Antarctic Volcanology Problems* (O. González-Ferrán, ed.), pp. 330–346, International Association of Volcanology and Chemistry of the Earth's Interior, Rome.

Barker, P. F. 1982. The Cenozoic subduction history of the pacific margin of the Antarctic Peninsula: Ridge crest-trench interactions, *J. Geol. Soc. London* **139**:787–801.

Barker, P. F., and Burrell, J. 1977. The opening of Drake Passage, *Mar. Geol.* **25**:15–34.

Barker, P. F., and Dalziel, I. W. D. 1983. Progress in geodynamics of the Scotia Arc region, in *Geodynamics of the Eastern Pacific Region, Caribbean and Scotia Arcs* (R. Cabre, ed.), Geodyn. Ser., Vol. 9, pp. 137–170, American Geophysical Union, Washington DC.

Barker, P. F., Dalziel, I. W. D., and Storey, B.C. 1992. Tectonic development of the Scotia arc region, in *Antarctic Geology* (R.J. Tingey, ed.), pp. 215–248, Oxford University Press, Oxford.

Birkenmajer, K. 1980. Age of the Penguin Island volcano, South Shetland Islands (West Antarctica) by the lichenometric method, *Bull. Acad. Pol. Sci. Ser. Sci. Terre* **27**:69–76.

Birkenmajer, K. 1992. Evolution of the Bransfield Basin and rift, West Antarctica, in *Recent Progress in Antarctic Earth Science* (Y. Yoshida, K. Kaminuma, and K. Shiraishi, eds.), pp. 405–410, Terra, Tokyo.

Birkenmajer, K., Delitala, M. C., Narebski, W., Nicoletti, M., and Petrucciani, C. 1986. Geochronology of Tertiary island-arc volcanics and glacigenic deposits, King George Island, South Shetland Islands (West Antarctica), *Bull. Acad. Pol. Sci. Ser. Sci. Terre* **34**:257–273.

Birkenmajer, K., and Keller, R. A. 1990. Pleistocene age of the Melville Peak volcano, King George Island, West Antarctica, by K-Ar dating, *Bull. Polish Acad. Sci., Earth Sci.* **38**:17–24.

Brault, M., and Simoneit, B. R. T. 1990. Mild hydrothermal alteration of immature organic matter in sediments from the Bransfield Strait, Antarctica, *Appl. Geochem.* **5**:149–158.

Dalziel, I. W. D. 1984. *Tectonic Evolution of a Forearc Terrane, Southern Scotia Ridge, Antarctica*, Geological Society of America Special Publication 200.

Fisk, M. R. 1990. Back-arc volcanism in the Bransfield Strait, Antarctica, *J. South Am. Earth Sci.* **3**:91–101.

Gambôa, L. A. P., and Maldonado, P. R. 1990. Geophysical investigations in the Bransfield Strait and in the Bellingshausen Sea, Antarctica, in *Antarctica as an Exploration Frontier: Hydrocarbon Potential, Geology and Hazards* (B. St. John, ed.), pp. 127–141, Am. Assoc. Petrol. Geol., Studies in Geology 31.

Garrett, S. W. 1990. Interpretation of reconnaissance gravity and aeromagnetic surveys of the Antarctic Peninsula, *J. Geophys. Res.* **95**:6759–6777.

Gonzalez-Ferran, O. 1985. Volcanic and tectonic evolution of the northern Antarctic Peninsula—late Cenozoic to recent, *Tectonophysics* **114**:389–409.

Gonzalez-Ferran, O. 1991. The Bransfield rift and its active volcanism, in *Geological Evolution of Antarctica* (M. R. A. Thomson, J. A. Crame, and J. W. Thomson, eds.), pp. 505–509, Cambridge Univ. Press, Cambridge.

Grad, M., Guterch, A., and Janik, T. 1993. Seismic structure of the lithosphere across the zone of subducted Drake plate under the Antarctic plate, West Antarctica, *Geophys. J. Int.* **115**:586–600.

GRAPE Team. 1990. Preliminary results of seismic reflection investigations and associated geophysical studies in the area of the Antarctic Peninsula, *Antarctic Sci.* **2**:223–234.

Guterch, A., Grad, M., Janik, T., and Perchuc, E. 1992. Tectonophysical models of the crust between the Antarctic Peninsula and the South Shetland trench, in *Geological Evolution of Antarctica* (M. R. A. Thomson, J. A. Crame, and J. W. Thomson, eds.), pp. 499–504, Cambridge University Press, Cambridge.

Guterch, A., Grad, M., Janik, T., Perchuc, E., and Pajchel, J. 1985. Seismic studies of the crustal structure in West Antarctica 1979–1980—Preliminary results, *Tectonophysics* **114**:411–429.

Guterch, A., Shimamura, H., and Polish–Japan–Argentina Research Group. 1991. An OBS-land refraction seismological experiment in the Bransfield trough, West Antarctica, 1990/1991: Abstracts, Sixth International Symposium on Antarctic Earth Sciences, 9–13 September, 1991, Japan, pp. 201–202.

Hawkins, J. W., Lonsdale, P. F., Macdougall, J. D., and Volpe, A. M. 1990. Petrology of the axial ridge of the Mariana Trough backarc spreading center, *Earth Planet. Sci. Lett.* **100**:226–250.

Hawkins, J. W., and Melchior, J. T. 1985. Petrology of Mariana Trough and Lau Basin basalts, *J. Geophys. Res.* **90**:11431–11468.

Herron, E. M., and Tucholke, B. E. 1976. Sea-floor magnetic patterns and basement structure in the southeastern Pacific, in *Init. Repts. DSDP*, 35 (C. D. Hollister and C. Craddock, *et al.*, eds.), pp. 263–278, U.S. Government Printing Office, Washington, DC.

Hickey-Vargas, R. 1992. A refractory HIMU component in the sources of island-arc magma, *Nature* **360**:57–59.

Hole, M. J., and Larter, R. D. 1993. Trench-proximal volcanism following ridge crest—trench collision along the Antarctic Peninsula, *Tectonics* **12**:897–910.

Hole, M. J., Rogers, G., Saunders, A. D., and Storey, M. 1991. Relation between alkalic volcanism and slab-window formation, *Geology* **19**:657–660.

International Seismological Centre Earthquake Catalogs. 1964–1993.

Irvine, T. N., and Baragar, W. R. A. 1971. A guide to the chemical classification of the common volcanic rocks, *Can. J. Earth Sci.* **8**:523–548.

Jeffers, J. D., and Anderson, J. B. 1990. Sequence stratigraphy of the Bransfield Basin, Antarctica: Implications for tectonic history and hydrocarbon potential, in *Antarctica as an Exploration Frontier: Hydrocarbon Potential, Geology and Hazards* (B. St. John, ed.), pp. 13–30, Am. Assoc. Petrol. Geol., Studies in Geology 31.

Jeffers, J. D., Anderson, J. B., and Lawver, L. A. 1991. Evolution of Bransfield basin, Antarctic Peninsula, in *Geological Evolution of Antarctica* (M. R. A. Thomson, J. A. Crame, and J. W. Thomson, eds.), pp. 481–485, Cambridge University Press, Cambridge.

Jin, Q., Kuang, F., Ruan, H., and Xing, G. 1991. Island arc volcanism and magmatic evolution in Fildes Peninsula, King George Island, Antarctica, Abstracts, Sixth International Symp. Antarctic Earth Sci., Ranzan, Japan, pp. 250–255.

Keller, R. A., and Fisk, M. R. 1992. Quaternary marginal basin volcanism in the Bransfield Strait as a modern analogue of the southern Chilean ophiolites, in *Ophiolites and Their Modern Analogues* (L. M. Parson, B. J. Murton, and P. Browning, eds.), pp. 155–170, Geol. Soc. Lond. Spec. Pub. No. 60.

Keller, R. A., Fisk, M. R., and Strelin J. A. 1993. Correlating distance from a trench with subducted component in recent basalts from the northern Antarctic Peninsula [abs.], *EOS* supplement, October 26, 1993, p. 663.

Keller, R. A., Fisk, M. R., White, W. M., and Birkenmajer, K. 1992. Isotopic and trace element constraints on mixing and melting models of marginal basin volcanism, Bransfield Strait, Antarctica, *Earth Planet. Sci. Lett.* **111**:287–303.

Keller, R. A., Strelin, J. A., Lawver, L. A., and Fisk, M. R. 1994. Dredging young volcanic rocks in Bransfield Strait, *Antarctic J. U.S.* **XXVIII**(1993 review issue):98–100.

Klepeis, K. A., and Lawver, L. A. 1994. Bathymetry of the Bransfield Strait, southeastern Shackleton fracture zone and South Shetland Trench, *Antarctic J. U.S.*, **XXVIII**(1993 review issue): 103–104.

Larter, R. D. 1991. Debate: Preliminary results of seismic reflection investigations and associated geophysical studies in the area of the Antarctic Peninsula, *Antarctic Sci.* **3**:217–222.

Larter, R. D., and Barker, P. F. 1989. Seismic stratigraphy of the Antarctic Peninsula Pacific margin: A record of Pliocene–Pleistocene ice volume and paleoclimate, *Geology* **17**:731–734.

Larter, R. D., and Barker, P. F. 1991. Effects of ridge crest-trench interaction on Antarctic–Phoenix spreading:forces on a young subducting plate, *J. Geophys. Res.* **96**:19,583–19,607.

Larson, R. L., and Chase, C. G. 1972. Late Mesozoic evolution of the western Pacific Ocean, *Geol. Soc. Am. Bull.* **83**:3627–3644.

Lawver, L. A., Dalziel, I. W. D., and Sandwell, D. T. 1993. Antarctic plate: tectonics from a gravity anomaly and infrared satellite image, *GSA Today* **3**:117–122.

Lawver, L. A., and Hawkins, J. W. 1978. Diffuse magnetic anomalies in marginal basins: Their possible tectonic and petrologic significance, *Tectonophysics* **45**:323–338.

Lawver, L. A., and Villinger, H. 1989. North Bransfield Basin: R/V POLAR DUKE cruise PD VI-88, *Antarctic J. Sci.* **23**:117–120.

Le Bas, M. J., La Maitre, R. W., Streckeisen, A., and Zanettin, B. 1986. A chemical classification of volcanic rocks based on the total alkali-silica diagram, *J. Petrol.* **27**:45–750.

Lin, P. N., Stern, R. J., Morris, J., and Bloomer, S. H. 1990. Nd- and Sr-isotopic compositions of lavas from the northern Mariana and southern volcano arcs: Implications for the origin of island arc melts, *Contrib. Mineral. Petrol.* **105**:381–392.

Maslanyj, M. P., Garret, S. W., Johnson, A. C., Renner, R. G. B., and Smith, A. M. 1991. Aeromagnetic anomaly of West Antarctica (Weddell Sea sector): BAS GEOMAP Series, Sheet 2, 1:2,500,000, with supplementary text, Cambridge, British Antarctic Survey.

Mayes, C. L., Lawver, L. A., and Sandwell, D. T. 1990. Tectonic history and new isochron chart of the South Pacific, *J. Geophys. Res.* **95**:8543–8568.

Nagihara, S., and Lawver, L. A. 1989. Heat flow measurements in the King George Basin, Bransfield Strait, *Antarctic J. Sci.* **23**:123–125.

Nelson, P. H. H. 1966. The James Ross Island Volcanic Group of north-east Graham Land, *Br. Antarct. Surv. Sci. Reports*, No. 54.

Pankhurst, R. J. 1983. Rb-Sr constraints on the ages of basement rocks of the Antarctic Peninsula, in *Antarctic Earth Science* (R. L. Oliver, P. L. James, and J. B. Jago, eds.), pp. 367–371, Austral. Acad. Sci., Canberra, and Cambridge Univ. Press, Cambridge.

Pankhurst, R. J., and Smellie, J. L. 1983. K-Ar geochronology of the South Shetland Islands, Lesser Antarctica: Apparent lateral migration of Jurassic to Quaternary island arc volcanism, *Earth Planet. Sci. Lett.* **66**: 214–222.

Parra, J. C., Gonzalez-Ferran, O., and Bannister, J. 1984. Aeromagnetic survey over the South Shetland Islands, Bransfield Strait and part of the Antarctic Peninsula, *Rev. Geol. Chile* **23**:3–20.

Pelayo, A. M., and Wiens, D. A. 1989. Seismotectonics and relative plate motions in the Scotia Sea region, *J. Geophys. Res.* **94**:7293–7320.

Renner, R. G. B., Sturgeon, L. J. S., and Garrett, S. W. 1985. Reconnaissance gravity and aeromagnetic surveys of the Antarctic Peninsula, *Br. Antarct. Surv. Sci. Rep.* No. 110.

Rex, D. C. 1976. Geochronology in relation to the stratigraphy of the Antarctic Peninsula, *Bull. Br. Antarct. Surv.* **43**:49–58.

Rex, D. C., and Baker, P. E. 1973. Age and petrology of Cornwallis Island granodiorite, *Br. Antarct. Surv. Bull.* **32**:55–61.

Roach, P. J. 1978. The nature of backarc extension in Bransfield Strait [abstract], *Geophys. J. R. Astron. Soc.* **53**:165.

Sandwell, T. T. 1992. Antarctic marine gravity field from high-density satellite altimetry, *Geophys. J. Int.* **109**:437–448.

Sandwell, D. T., and Smith, W. H. F. 1992. Global marine gravity from ERS-1 Geosat and Seasat reveals new tectonic fabric, *EOS Trans. AGU* **73**:133.

Saunders, A. D., and Tarney, J. 1984. Geochemical characteristics of basaltic volcanism within backarc basins, in *Marginal Basin Geology: Volcanic and Associated Sedimentary and Tectonic Processes in Modern and Ancient Marginal Basins* (B. P. Kokelaar and M. F. Howells, eds.), pp. 59–76, Geol. Soc. Sp. Pub. No. 16.

Saunders, A. D., Tarney, J., and Weaver, S. D. 1980. Tranverse geochemical variations across the Antarctic Peninsula: Implications for the genesis of calc-alkaline magmas, *Earth Planet. Sci. Lett.* **46**:344–360.

Saunders, A. D., Weaver, S. D., and Tarney, J. 1982. The pattern of Antarctic Peninsula plutonism, in *Antarctic Geosciences* (C. Craddock, ed.), pp. 305–314, University of Wisconsin Press, Madison.

Schlosser, P., Suess, E., Bayer, R., and Rhein, M. 1988. ^{3}He in the Bransfield Strait waters: Indication for local injection from backarc rifting, *Deep-Sea Res.* **35**:1919–1935.

SEAN. 1993. Scientific Event Alert Network Bulletin for 31 March 1993, Smithsonian Institute, Washington, DC, p. 8.

Silfer, J. A., Engel, M. H., and Macko, S. A. 1990. The effect of hydrothermal processes on the distribution and stereochemistry of amino acids in recent Antarctic sediments, *Appl. Geochem.* **5**:159–167.

Simoneit, B. R. T. 1983. Effects of hydrothermal activity on sedimentary organic matter: Guaymas Basin, Gulf of California—Petroleum genesis of protokerogen degradation, in *Hydrothermal Processes at Seafloor Spreading Centers* (P. A. Rona, K. Bostrom, L. Laubier, and K. L. Smith, eds.), pp. 451–471, Plenum, New York.

Smellie, J. L. 1983. A geochemical overview of subduction-related igneous activity in the South Shetland Islands, Lesser Antarctica, in: *Antarctic Earth Science* (R. L. Oliver, P. L. James, and J. B. Jago, eds.), pp. 352–356, Austral. Acad. Sci., Canberra, and Cambridge Univ. Press, Cambridge.

Smellie, J. L. 1987. Geochemistry and tectonic setting of alkaline volcanic rocks in the Antarctic Peninsula: A review, *J. Volcanol. Geotherm. Res.* **32**:269–285.

Smellie, J. L. 1988. Recent observations on the volcanic history of Deception Island, South Shetland Islands, *Br. Antarct. Surv. Bull.* **81**:83–85.

Smellie, J. L. 1990. D. Graham Land and South Shetland Islands, in *Volcanoes of the Antarctic Plate and Southern Oceans* (W. E. LeMasurier and J. W. Thomson, eds.), pp. 302–359, Antarct. Res. Ser., American Geophysical Union, Washington, DC, 48.

Smellie, J. L., Davies, R. E. S., and Thomson, M. R. A. 1980. Geology of a Mesozoic intra-arc sequence on Byers Peninsula, Livingston Island, South Shetland Islands, *Br. Antarct. Surv. Bull.* **50**:55–76.

Smellie, J. L., Pankhurst, R. J., Hole, M. J., and Thomson, J. W. 1988. Age, distribution and eruptive conditions of late Cenozoic alkaline volcanism in the Antarctic Peninsula and eastern Ellsworthland: Review, *Br. Antarct. Surv. Bull.* **80**:21–49.

Smellie, J. L., Pankhurst, R. J., Thomson, M. R. A., and Davies, R. E. S. 1984. The Geology of the South Shetland Islands. VI: Stratigraphy, Geochemistry and Evolution, *Br. Antarct. Surv. Sci. Rep.* No. 87.

Stern, C. R., Frey, F. A., Futa, K., Zartman, R. E., Peng, Z., and Kyser, T. K. 1990. Trace-element and Sr, Nd, Pb, and O isotopic composition of Pliocene and Quaternary alkali basalts of the Patagonian Plateau lavas of southernmost South America, *Contrib. Min. Petrol.* **104**:294–308.

Strelin, J. A., Carrizo, H., Lopez, A., and Torielli, C. 1993. Actividad volcanica holocena en la Isla James Ross. *Segundas Jornadas de Comunicaciones sobre investigaciones Antarticas, Actes* pp. 335–340, Buenos Aires.

Suess, E., Fisk, M., and Kadko, D. 1988. Thermal interaction between backarc volcanism and basin sediments in the Bransfield Strait, Antarctica, *Antarctic J. U. S.* **22**(5):46–49.

Sykes, M. A. 1988. New K-Ar age determinations on the James Ross Island Volcanic Group, north-east Graham Land, Antarctica, *Brit. Antarct. Surv. Bull.* **80**:51–56.

Tanner, P. W. G., Pankhurst, R. J., and Hyden, G. 1982. Radiometric evidence for the age of the subduction complex of the South Orkney and South Shetland Islands, West Antarctica, *J. Geol. Soc. Lond.* **139**:683–690.

Thomson, M. R. A. 1992. Stratigraphy and age of pre-Cenozoic stratified rocks of the South Shetland Islands: review, in *Geologia de la Antartida occidental* (J. Lopez-Martinez, ed.), pp. 75–92, Simposios T3, III Congreso Geologico de Espana y VIII Congreso Latinamericano de Geologica, Salamanca.

Vila, J., Ortiz, R., Correig, A. M., and Garcia, A. 1992. Seismic activity on Deception Island, in *Geological evolution of Antarctica* (M. R. A. Thomson, J. A. Crame, and J. W. Thomson, eds.), pp. 449–456, Cambridge University Press, Cambridge.

Weaver, S. D., Saunders, A. D., Pankhurst, R. J., and Tarney, J. 1979. A geochemical study of magmatism associated with the initial stages of backarc spreading: The Quaternary volcanics of the Bransfield Strait from South Shetland Islands, *Contrib. Mineral. Petrol.* **68**:151–169.

Weaver, S. D., Saunders, A. D., and Tarney, J. 1982. Mesozoic-Cenozoic volcanism in the South Shetland Islands and the Antarctic Peninsula: Geochemical nature and plate tectonic significance, in *Antarctic Geoscience* (C. Craddock, ed.), pp. 263–273, Univ. Wisconsin Press, Madison.

Wernicke, B. 1981. Low-angle normal faults in the Basin and Range province: Nappe tectonics in an extending orogen, *Nature* **291**:645–648.

Whiticar, M. J., Suess, E., and Wehner, H. 1985. Thermogenic hydrocarbons in surface sediments of the Bransfield Strait, Antarctic Peninsula, *Nature* **314**:87–90.

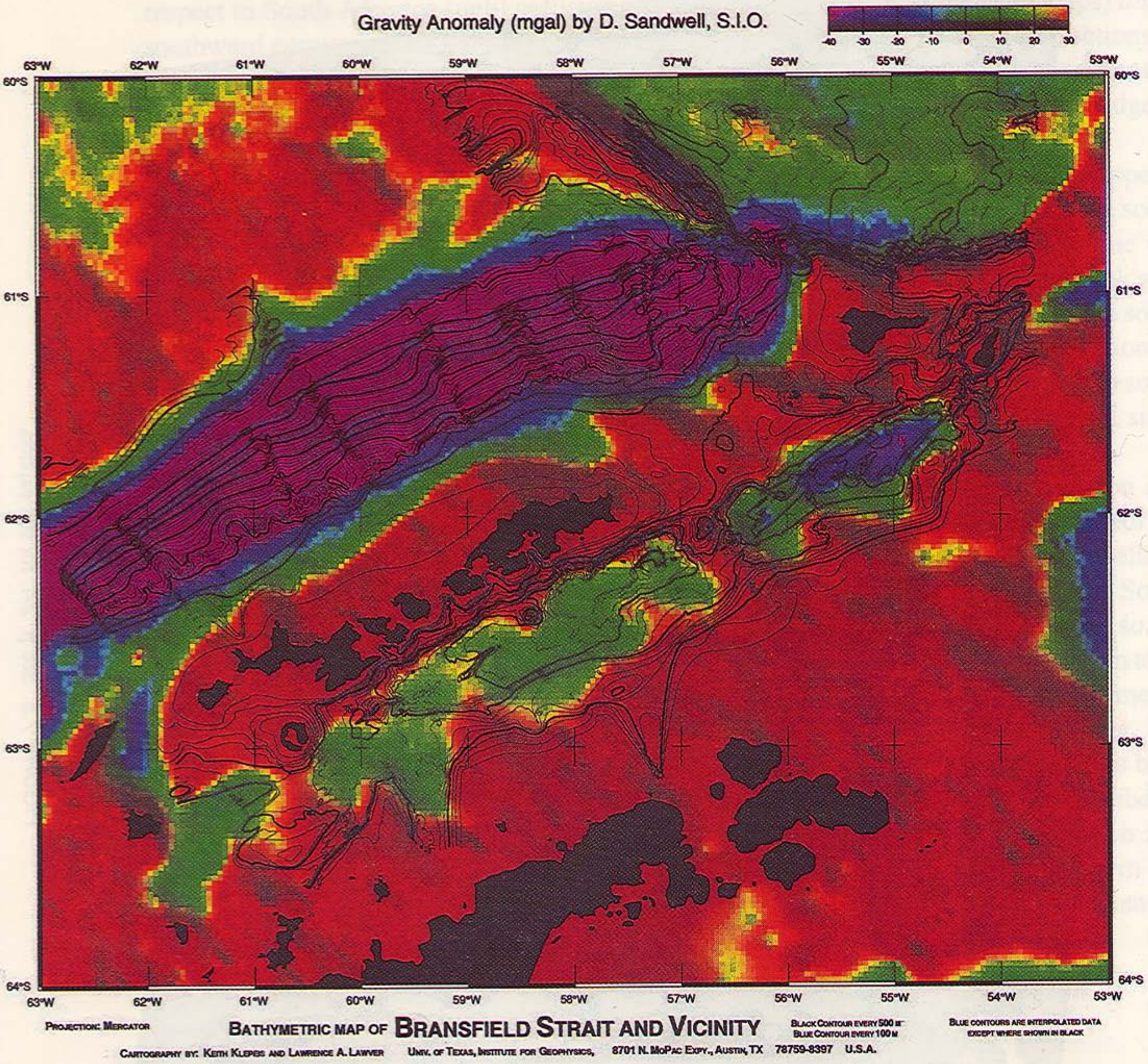

FIGURE 8.5. Geostat/ERS-1 gravity data from Sandwell and Smith (1992) with digital bathymetric data of Klepeis and Lawver (1994) superimposed. The gravity data color bar indicates gravity values from <-40 mgal to $>+30$ mgal. Bold black bathymetric contours are shown every 500 m, while thin black contours are observed bathymetry contoured every 100 m. Thin blue contours are interpolated bathymetric data contoured every 100 m.